ETH Zurich – 15 dec. 2011 Colloquium on seismic design of tunnels

Design of underground structures under seismic conditions: a long deep tunnel and a metro tunnel.

Moreno Pescara, Giuseppe Maria Gaspari, Luca Repetto
Geodata Engineering SpA, Torino, Italy

1 INTRODUCTION

Tunneling is increasingly being seen as an environmentally preferable means of providing infrastructure to densely populated urban areas as well as for long transportation infrastructures, thus posing a number of challenging conditions.

Historically, underground facilities have experienced a lower rate of damage than surface structures. Nevertheless, some underground structures registered significant damages in recent large earthquakes; the resultant databases which can be found in literature, together with the quite slight overburden of many stretches of the metro line, required a particular care on the verification of the vulnerability of the underground structures under severe seismic events. Moreover, also long and deep tunnels are more and more required to be designed against seismic event by the Client.

This article describes briefly the main assessments on the approaches used by engineers in quantifying the seismic effect on an underground structure, both referring to deterministic either probabilistic methods. However, the main purpose is that of proposing a new simplified approach to evaluate through numerical simulations the ovaling effect on the cross sections of tunnels. This method could be applicable not only to obtain closed form solutions for circular shapes, but also to acquire the stresses acting on the lining of tunnels characterized by complex geometries and non homogeneous ground conditions. Therefore, this study has the goal to propose a method that could be as more consistent as possible with the common procedures nowadays adopted to evaluate the effect of seismic motion on tunnels in a way that can be reliable for structures subjected to ground motion caused by a seismic event. Of course, the method cannot be apply to those conditions where a fault zone is close to the structure or they cross each other.

After a short presentation of the theoretical approach followed, the paper deals with the case of Istanbul Metro line Kadikoy-Kartal and the T74R railway tunnel along the line from Dharam to Qazigund in Kashmir region of India.

2 GENERAL SEISMIC DESIGN PROCEDURES

The ground strain and the curvature due to wave propagation influence the response of the tunnels. The motion of the soil particle depends on the type of waves, but can always be resolved into a longitudinal and transverse component with respect to the tunnel and immersed tube axis. The propagation velocity of the body and surface waves along the alignment (apparent velocity of propagation) and the peak ground velocity are the two important parameters that control wavelength and amplitude. The maximum ground curvature will be equal to the second derivative of the transverse displacement with respect to distance and is controlled by the peak ground acceleration transverse to the direction of wave propagation and the apparent velocity of propagation. In present section the most common methods to evaluate the effects of ground motion on underground structures will be briefly summarized.

2.1 *Ground deformation approach*

The general procedure for seismic design of tunnel structures is based primarily on the ground deformation approach. During earthquakes, tunnel structures are assumed to move together with the surrounding soil media. The structures, therefore, are designed to accommodate the deformations imposed by the ground. However, the effects of soil structure interaction can play an important role in the seismic response of tunnel or over buried structures, particularly when the structure is surrounded by soft media (such as the case for an immersed tunnel) and therefore should be considered in the analysis. Furthermore, for tunnel structures with considerable structural discontinuities (such as joints between tunnel segments and between the tunnel and the station structure) detailed evaluations have to be given to the effects of these discontinuities on the earthquake resistance of the tunnel.

Earthquake resistant design for buried structure:

In all cases the earthquake excitation can be represented by a vertically propagating horizontally polarized shear wave incident from the engineering bedrock (NEHRP B/C boundary).

An underground tunnel structure undergoes three primary modes of deformation during seismic shaking (Fig. 1):

- ovaling deformation;
- axial deformation;
- curvature deformation.

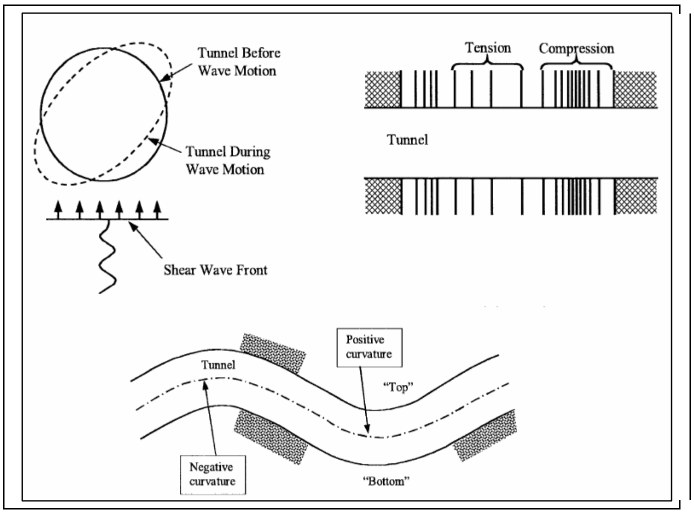

Figure 1. Primary deformation modes of tunnels due to seismic shaking [Owen and Scholl, 1981].

The ovaling deformation is caused primarily by seismic waves propagating perpendicular to the tunnel longitudinal axis. The axial and curvature deformations are induced by components of seismic waves that propagate along the longitudinal axis and/or by spatially varying ground motions resulting from local soil/site effects. Wave propagation strains tend to be most pronounced at the junctions of dissimilar buried structures (such as tunnel connecting with a building) or at the interfaces of different geologic materials (such as passing from rock to soft soil).

2.2 *Application of the free-field shear deformation method*

The methodology of the seismic loading design is in that basic design loading criteria (static condition) has to incorporate the additional loading imposed by ground shaking and deformation. In general seismic design loads for tunnel are characterized in terms of the deformations and strains imposed on the structure by the surrounding ground based on their interaction. To describe procedure used to compute deformations and force corresponding to the three deformations modes, two design approaches have been introduced as:

- Free-field deformation approach [Wang 1996; Power et al. 1998; Hashash et al. 2001]
- Soil- structure interaction approach

In free-field deformation approach, the ground deformation caused by seismic waves is assumed to occur in the absence of structure or excavation. Theses deformations ignore the interaction between the underground structure and the surrounding ground, but can provide a first-order estimate of the anticipated deformation of the structure. The closed form elastic solution results in combined axial and curvature deformations, assuming the tunnel as an elastic beam and maximum strain at critical incidence angle. The advantages and disadvantages of this method have been reported by Wang (1993). The presence of an underground structure modifies the free-field ground deformations; so a method based on soil-structure interaction is required. This solution uses the beam-on-elastic foundation approach that is used to model (quasi-static) soil-structure interaction effects. Under seismic loading, the cross-section of a tunnel experiences axial bending and shear strains due to free-field axial, curvature, and shear deformations as illustrated in Fig. 2.

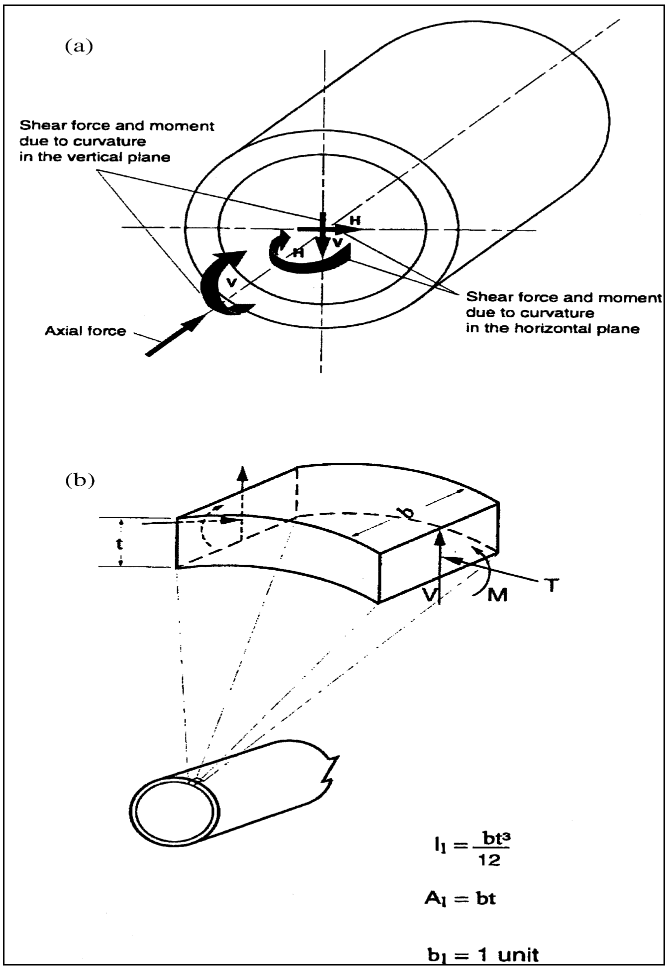

Figure 2. Induced forces and moments caused by seismic waves [Power et al., 1996], (a) Induced forces and moments caused by waves propagating along tunnel axis. (b) Induced circumferential forces and moments caused by waves propagating perpendicular to tunnel axis.

The closed form solutions for estimating ground-structure interaction for tunnels are generally based on the assumptions that:

- The shape of the tunnel is circular,
- The ground is an infinite, elastic, homogeneous, isotropic medium,
- The circular lining is generally an elastic, thin walled tube under plane strain conditions,
- Full-slip or no-slip conditions exist along the interface between the ground and the lining,
- Loading conditions are simulated as external loading.

The following chapter describes the approach adopted for the simulation of the seismic effects taking the advantage of using numerical analysis in order to overcome some limitations related to the complex geometry of tunnel sections, as shown in previous chapters.

3 ADOPTED SEISMIC DESIGN AND VERIFICATION PROCEDURES

The approach used to examine the effect of the seismic actions on the tunnel stability is the free-field shear deformation method [Wang, 1993, Power et al. 1998; Hashash et al. 2001], which represent the most conservative condition. This approach assumes that the deformation of the structure should conform to the deformation of the soil in the free-field under the design earthquakes.

This section of the paper presents the methodology applied to evaluate the ovaling effect on the analyzed tunnels: after an evaluation of the expected shear deformation on the structure in free field conditions, it was applied to the numerical model in order to reproduce the ovaling of the lining. Finally, dimensioning and verification of the steel reinforced structures had been made by an application of Eurocode coefficient to the stresses evaluated in the analysis.

3.1 *Evaluation of the maximum shear deformation in free field condition*

The applied methodology foresaw the application of a deformation to the ground so as to deform the underground structures and obtain the stresses acting in the final lining in case of a seismic event.

The starting point of the study is given by the knowledge of the Peak Ground Acceleration (PGA, here a_{gR}), which is given by the local norms or by specific studies.

It must be highlighted that what is needed is the PGA at a rigid bedrock, otherwise the application of the soil factor S according to EC8 (cfr eq. 1) is not valid.

The site-specific Peak Ground Acceleration ($a_{max,s}$) is given by the equation (2), where S is the soil factor, defined in terms of the ground type [Eurocode 8]:

$$a_{\max,s} = S \cdot a_{gR} \qquad (1)$$

The value of S, suggested in Eurocode 8, is based on the types of elastic response spectra. In Tables 1 the S values are characterized by Mw<5.5 and Mw>5.5, respectively:

- Table 1.a refer to conditions characterized by Mw < 5.5
- Table 1.b refer to conditions characterized by Mw $\geq$ 5.5

Ground type	S	T_B (s)	T_C (s)	T_D (s)
A	1,0	0,05	0,25	1,2
B	1,35	0,05	0,25	1,2
C	1,5	0,10	0,25	1,2
D	1,8	0,10	0,30	1,2
E	1,6	0,05	0,25	1,2

Table 1.a. Values of the parameters describing the recommended Type 1 elastic response spectra [Eurocode].

Ground type	S	T_B (s)	T_C (s)	T_D (s)
A	1,0	0,15	0,4	2,0
B	1,2	0,15	0,5	2,0
C	1,15	0,20	0,6	2,0
D	1,35	0,20	0,8	2,0
E	1,4	0,15	0,5	2,0

Table 1.b. Values of the parameters describing the recommended Type 2 elastic response spectra [Eurocode].

In order to consider the depth of the tunnels, a simplified procedure [Hashash et al., 2001] was considered to define the peak acceleration at the depth of the tunnel $a_{z,max}$: this consists in the determination of a reduction coefficient C for the peak acceleration on the surface depending on the depth of the tunnel (Table 2) as for equation (2):

$$a_{z,\max} = C \cdot a_{\max s} \quad (2)$$

where $a_{z,max}$ is the peak acceleration at the depth of the tunnel.

Tunnel depth (m)	Ratio of ground motion at tunnel depth to motion at ground surface
≤ 6	1.0
6–15	0.9
15–30	0.8
> 30	0.7

Table 2. Ratios of ground motion (C) at depth to motion at ground surface [Power et al. 1996].

The value of $a_{z,max}$ is used to determine the γ_{max} (maximum shear deformation in free-field condition) from the peak ground velocity V_s (Table 2) that is a function of earthquake magnitude and distance from the seismic source, as shown in equations (3) and (4):

$$\gamma_{\max} = \frac{V_s}{C_s} \quad (3)$$

$$V_s = k \cdot a_{z,\max} \quad (4)$$

where k is the ratio of peak ground velocity to peak ground acceleration, obtained from Table 3; Cs is the apparent propagation velocity of S-wave.

Moment magnitude (M_w)	Ratio of peak ground velocity (cm/s) to peak ground acceleration (g)		
	Source-to-site distance (km)		
	0–20	20–50	50–100
Rock[a]			
6.5	66	76	86
7.5	97	109	97
8.5	127	140	152
Stiff soil[a]			
6.5	94	102	109
7.5	140	127	155
8.5	180	188	193
Soft soil[a]			
6.5	140	132	142
7.5	208	165	201
8.5	269	244	251

[a] In this table, the sediment types represent the following shear wave velocity ranges: rock ≥ 750 m/s; stiff soil is 200–750 m/s; and soft soil < 200 m/s. The relationship between peak ground velocity and peak ground acceleration is less certain in soft soils.

Table 3. Ratios of pick ground velocity to pick ground acceleration in different grounds and for increasing source-to-site distance [Power et al. 1996].

The apparent propagation velocity of S-wave (C_s) is not necessarily equal to the real propagation velocity; in fact, several authors [O'Rourke & Liu, 1999; Power et al., 1996; Paolucci & Pitilakis, 2007] have suggested values between 1 and 5km/s.

The value of γ_{max} corresponds to the maximum horizontal displacement imposed in the numerical model, calculated as per equation (5):

$$\Delta x \max = \gamma_{\max} \cdot \left(\frac{h_{\mathrm{mod}}}{2} \right) \tag{5}$$

where h_{mod} is the height of the model and Δx_{max} is the horizontal displacement applied to the model.
In this way, Δx_{max} is obtained applying to the sides of the model punctual forces in order to generate a rotation of the entire model (Fig. 3) and consequently the ovaling effect of the excavation boundary, as shown in Fig.4.

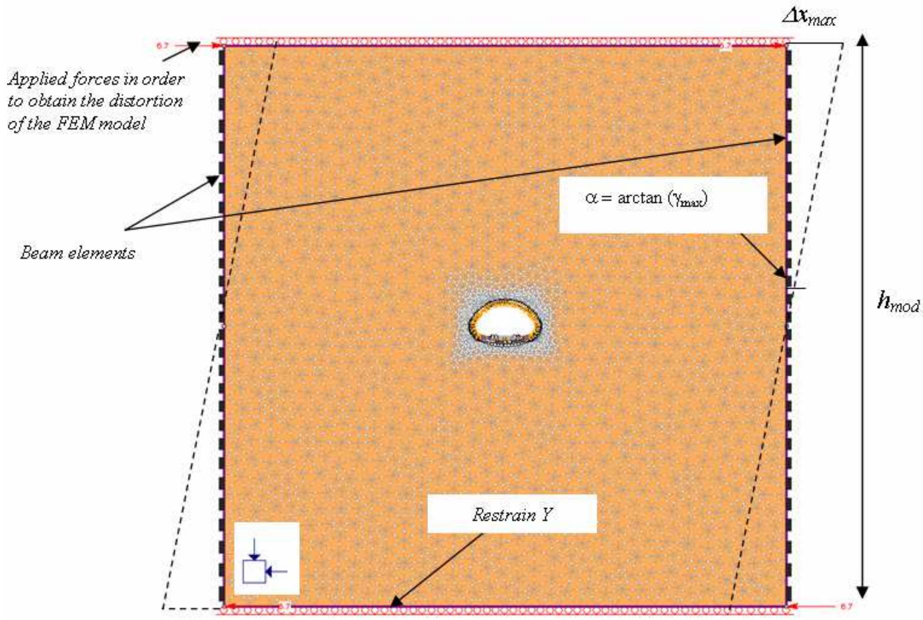

Figure 3. Numerical model for the application of the Free-Field Shear Deformations Method.

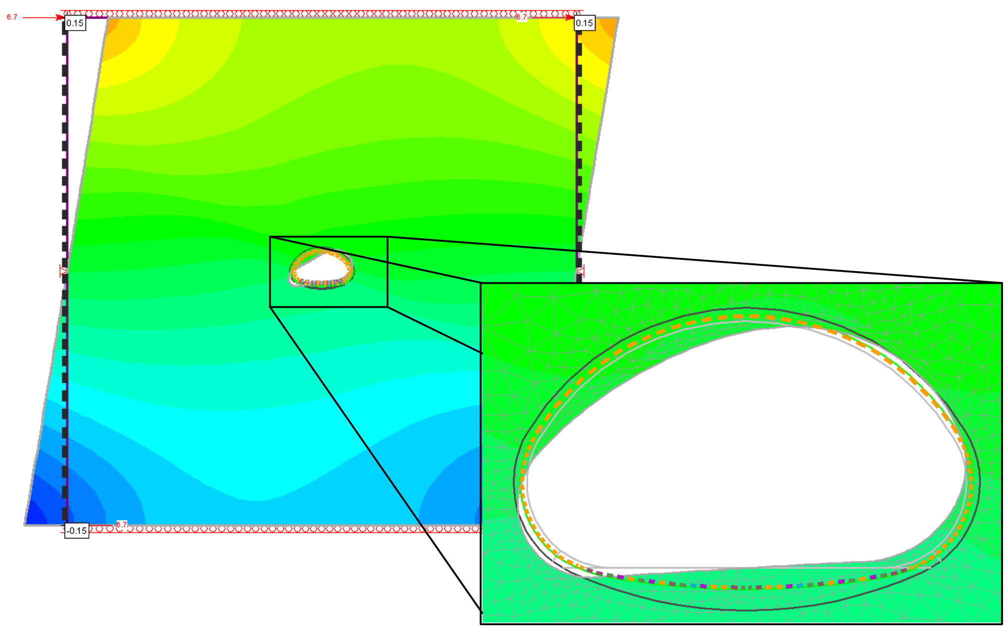

Figure 4. Ovaling Effect of the excavation boundary.

With this methodology it was possible to find the stresses, due to the ovaling deformations, acting in the underground final structures for the cases of the design earthquakes.

3.2 *Modelling of the ovaling effect with finite elements analysis*

A series of computational analyses using finite element code (Phase2 - v6, RocScience) were performed in order to verify the proposed procedure in the previous section and to properly calibrate the model, so to get same results for a circular shaped tunnel as from simplified methods with closed form solutions [Barla et al., 1986; Wang, 1993; Bobet, 2003;Corigliano et al., 2008].

The mesh and the lining-ground system used in these analyses are shown in Figure 2. The assumptions made for these analyses include the following:

- Plane strain model with no gravity loading was performed.
- No water pressure and no flow boundary conditions were assumed in the model.
- Seismic shear wave loading is simulated by pure shear conditions, through a "trial & error procedure", by applying horizontal line-forces to the upper and lower external boundaries of the model, thus checking whether the obtained horizontal displacement Δx_{max} was the desired one or further analyses are required to achieve it.

The Authors verified that the direct application of the displacement field to the mesh rather than a force distribution could not allow a proper evaluation of the real effects in terms of stresses on the tunnel lining.

- In order to make possible the rigid distortion of the model and to create a pure shear condition, high strength liners were modelled at the vertical external borders and a hinge was created on both sides at an height of h/2. Hinges were introduced in order to create a proper restraint that can avoid numerical errors due to eventual fictitious horizontal translations.
- As the geometry of the cross sections (particularly of the switches, exemplified in this article) is not regular, no advantage of the anti-symmetric loading conditions could be taken, thus the entire lining/ground system was analysed.
- Lining was modelled by a series of continuous flexural beam elements of linear elasticity, as described below. The hypothesis of an elastic dominion for the structure is a conservative way to take into account the difficult evaluation of the activation and evolution of plastic hinges.
- Due to its high stiffness, subsoil layers were modelled as a linear elastic homogeneous and isotropic material.
- No-slip condition along the lining-ground interface is assumed as it is recognised the most suitable for rock formations and for a proper simulation of waterproofing.
- Mechanical parameters implemented in the model were derived directly from the information given by field tests and laboratory studies on the specimens taken from the borehole. Correlations found in literature were considered and compared: as for the elastic modulus, Stacy correlation was adopted, a ratio $E_{dyn}/E_{static}=2$ was used, with: E_{dyn} = dynamic modulus of the equivalent material used for numerical analyses and E_{static} = elastic Young modulus measured with site testing (pressure-meter) on the rock mass.

Some more words should be spent as to describe the final lining modelling. The final lining will be simulated trough elastic material elements and beam elements ("Equivalent Axis Beam Method").

The forces acting on the final lining are obtained directly adopting this methodology which foresee to define, on the axis line of the final lining, a number of beam elements characterized by:

Beam thickness = thickness of the final lining.
Beam modulus = concrete modulus divided by a factor of scale F, with $F=10^{10}$.

Due to their very low stiffness values, the beam elements deform as the final lining material (without interfering with the stress and strain fields inside the final lining material elements).

The stress values obtained on the beam elements are scaled by a factor equal to F, so that, when coming to the dimensioning phase, it is necessary to multiply them by the same factor in order to obtain a proper verification.

A short description of this method is shown in Fig. 5.

The main advantages of this methodology are the following:

- more homogeneous and more detailed results for the final lining stresses;

- possibility to verify quicker all the beams (ensuring that all the final lining is verified);
- axial force (N), bending moment (M) and thrust force (V) are obtained directly from the analyses avoiding results integration, which often induces many mistakes;
- possibility to plot directly the values of N, M and V: in this way a quick visual check of the forces and bending moments distribution is possible.

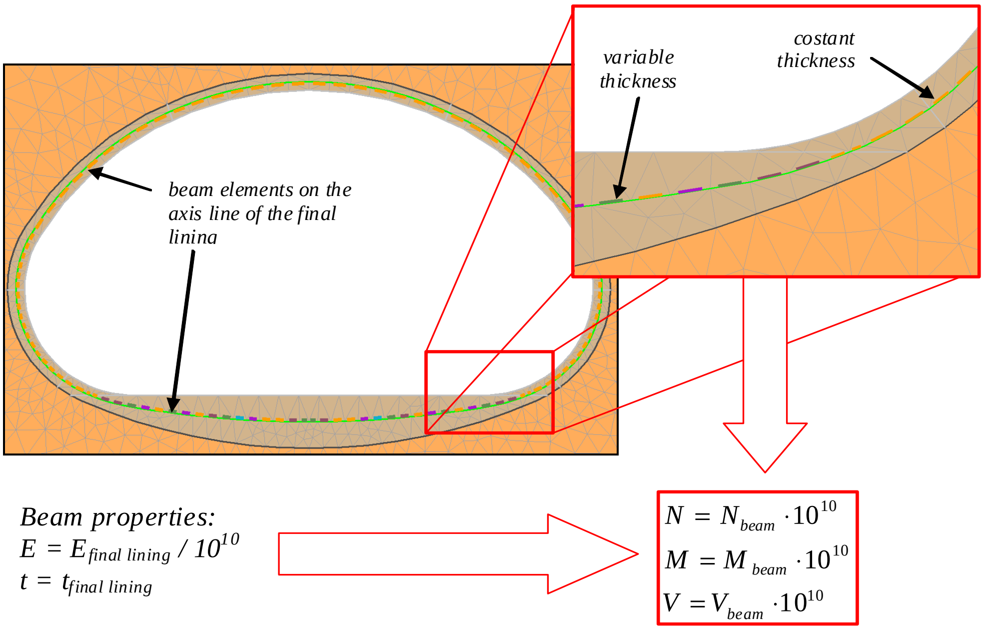

Figure 5. Equivalent Axis Beam Method for the final lining of Metro Istanbul – Kadikoy-Kartal line.

3.3 *Dimensioning and verifications on the final lining*

The numerical analyses have been chosen to dimension the final lining in static and seismic condition with and without water pressure.

In order to verify the final lining under static and seismic load conditions (with and without water pressure) different loading combinations have been investigated through FEM and structural numerical simulations, with the hyperstatic reaction method.

Three typologies of numerical analyses are have been performed, as shown in Table 4.

Analysis	*Description*	*Induced Stresses*
A	*FEM Analysis in static condition without water pressure*	*S(g)*
B	*FEM Analysis in static condition with water pressure*	*S(g) + S(w)*
C	*Pseudo-Static FEM Analysis (Free Field Method – Ovaling effect) without water pressure*	*ΔS(g)*

S(g): Stress function of the field stress

S(w): Stress function of the water pressure

ΔS(g): Increase of stress function of the field stress

Table 4. Numerical analysis typologies.

Table 5 shows the six different loading combinations based on the previously mentioned analysis. In the seismic conditions, the internal forces obtained from A (or B) simulations have been summed to the internal forces obtained from C analysis, as for the common known method of superposition of the effects of the actions.

	Static Condition	Seismic Condition
Dry condition	A	A+C
Saturated condition	B	B+C

Table 5. Loading combinations.

The structural verifications are performed according to EN 1992 [Eurocode 2] for Ultimate Limit State (U.L.S.) and Serviceability Limit State (S.L.S.), except for the seismic case in which this last one is not required. The structural analyses were performed in order to demonstrate the final lining adequateness in terms of geometry, thickness and reinforcement.

Structural verification for Ultimate Limit State (U.L.S.)

As for the U.L.S. verifications, for the final lining verification α, that is a factor taking into account for the effects of long duration loads, is considered equal to 0.85 [EC2, paragraph 3.1.6].

The axial force, bending moment and shear forces values, which were obtained directly from the numerical analyses, were multiplied by a factor γ_G, as shown in equations (6):

$$N_d = \gamma_G \cdot N_k$$
$$M_d = \gamma_G \cdot M_k$$
$$V_d = \gamma_G \cdot V_k \qquad (6)$$

For the bending moment - axial force verification, the resistance envelope for the final lining is obtained according with formulations (7) and (8):

$$f_{cd} = \frac{\alpha \cdot 0.83 \cdot R_{ck}}{\gamma_c} = \frac{\alpha \cdot f_{ck}}{\gamma_c} \qquad (7)$$

$$f_{yd} = \frac{f_{yk}}{\gamma_s} \qquad (8)$$

Where: γ_c is a resistance reduction factor for the concrete

γ_s is a resistance reduction factor for the steel

Refer to Table 6 in order to review a summary of the considered input data for the S.L.U. verifications and all the corresponding adopted coefficients.

	Bending Moment – Axial Force Verification			*Shear Force Verification*		
	Static condition	*Seismic condition*		*Static condition*	*Seismic condition*	
		S1 PGA_475	S2 PGA_2475		S1 PGA_475	S2 PGA_2475
γ_G	1.35	1.0	1.0	1.35	1.0	1.0
γ_c	1.5	1.5	1.0	1.5	1.5	1.0
γ_s	1.15	1.15	1.0	1.15	1.15	1.0

PGA_475 = *peak ground acceleration refers to average return period of 475 years*
PGA_2475 = *peak ground acceleration refers to average return period of 2475 years*
γ_G = *amplification factor of loads [EC1, paragraph 9.4.3]*
γ_c = *resistance reduction factor for the concrete [EC2, paragraph 2.4.2.4]*
γ_s = *resistance reduction factor for the steel [EC2, paragraph 2.4.2.4]*

Table 6. Summary of the considered input data and factors for the Ultimate Limit State verifications for the case of Istanbul Metro.

Structural verification for Serviceability Limit State (S.L.S.)

For the S.L.S., the structural analyses consist in verifying that the width of the crack w is less than 0.3mm. In the same way the maximum stress must be always lower than the allowable stress for concrete and steel.

In detail, the maximum compressive stress for the concrete and for the steel is obtained as:

$f_{c,SLS} = 0.6 \cdot f_{ck}$ [EC2, paragraph 7.2]

$f_{y,SLS} = 0.8 \cdot f_{yk}$ [EC2, paragraph 7.2]

For the seismic condition, the S.L.S. verification is not required, so that it won't be shown in this article, but it was necessary to verify the Static conditions of the final lining.

4 A LONG AND DEEP TUNNEL: THE CASE OF T74R IN INDIA

4.1 *The Railways line*

IRCON INTERNATIONAL LIMITED (IRCON), Government of India Undertaking, under Ministry of Railways has been entrusted with the design and construction of New Broad Gauges Railway line from Dharam – Qazigund section (km 100.8 to km 168 along the old alignment) of Udhampur–Srinagar-Baramulla BG Rail Link Project in the state of Jammu & Kashmir in Northern India. This stretch is part of the USBRL project (Fig. 6).

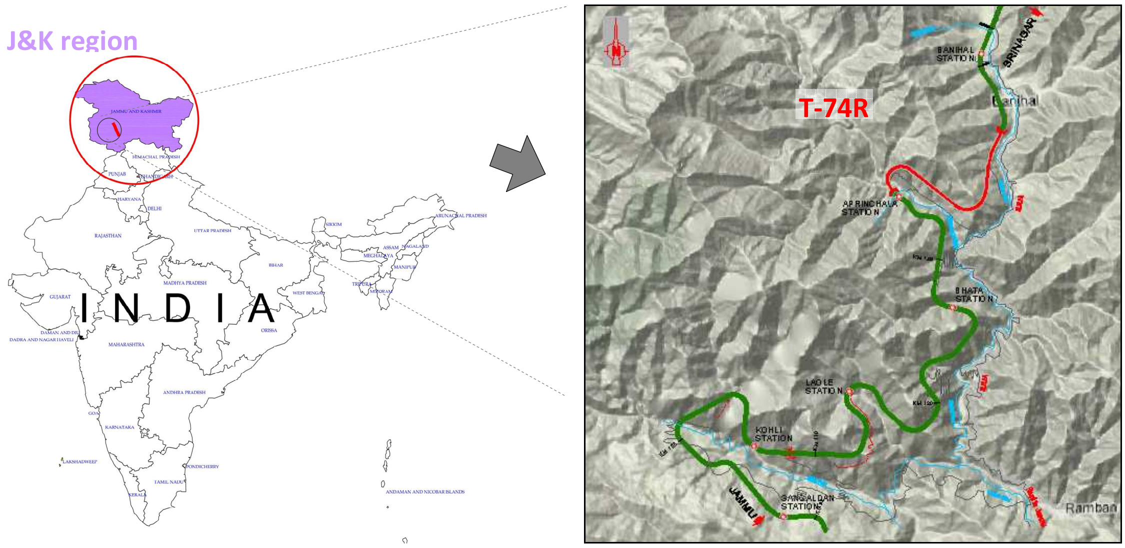

Figure 6 (left) plan view of India with indication of J&K region in violet and location of the USBRL Project in red; (right) plan view of USBRL Project in green in the zone of Banihal while in red it is reported the location of the New T-74R tunnel

The mining of T-74R on a new deeper alignment compared to the original one, has been due to the geological problems encountered during the excavation of the shallow T-67/T-68 and T-73/T-74 tunnels. The T-74R tunnel has length of 8.6km and by-passes from the km 134 to the km 145 of the old alignment. The new tunnel will be excavated between the right side of the Bishlari river valley (roughly 5 km downstream and southward of Banihal) and the last 5 km of the left hillside of its tributary, the valley of the Mahumangat Nalla

4.2 *T74R tunnel*

Considering the general layout of the problem with a portion of tunnel to be re-used and the safety lay-out to be defined, a Multi Criteria Analysis has been developed based on the following four schematic alternatives (Table. 7) .

Table 7 – Comparison of alternatives

	← Katra	Scheme of tunnel system	Srinagar →	Reference cross section	Elements	Note
Solution A		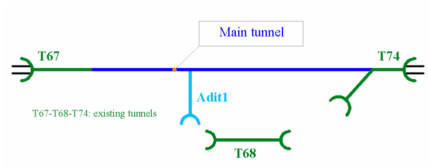		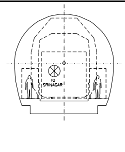 Area=38.2m^2	Single-tube, Single-track with 1 adit	-
Solution B		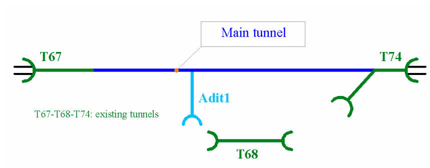		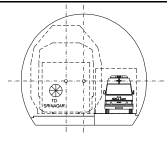 Area=51.8m^2	Single-tube, Single-track with 1 adit	With motorable way (as Pir Panjal tunnel: no examples of this cross-section are available in Europe)
Solution C		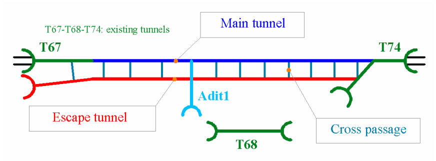		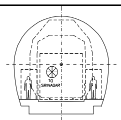 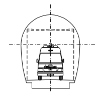 Area=38.2m^2 Area=18.5m^2	Single-tube, Single-track, Separate sidewalk for escape	Minimum requirements as per safety standards
Solution D		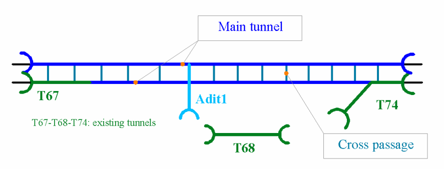		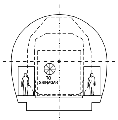 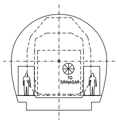 Area=38.2m^2 Area=38.2m^2	Double tube, Single track	-

Among all these one the selection was made for alternative C and finally the characteristics of the chosen solution are listed below

- Main Tunnel length = 8610 m (from T-67 South portal: P1, CH 125+313.11 to T-74 North portal: P2, CH 133+901.43 equivalent to the old CH 145+683); Finished Cross sectional Area: 38.2 m2; finished Cross sectional Area (existing T-67): 48.0 m2; excavated Cross sectional Area: from 58 m2 to 73 m2.
- Maximum gradient: 1.25% compensated.
- Design Speed of 100 km/hour.
- Minimum curvature radius: 445 m.
- Maintenance niche (MN): No. 33, each at L = 250m distance.
- Trolley refuge niche (TR): No. 83, each at L = 100m distance; size of Trolley refuge will be 3.40 m X 3.45 m x3.40 m; for visibility reasons Trolley refuge will be located always on the external side of the curves.
- Safety and Escape Tunnel length = 7407 m (from Safety and escape tunnel South portal to Cross passage type B No.7); finished cross sectional area of Escape Tunnel will be 18.2 m2; excavated Cross sectional area of Escape Tunnel will be 28 to 32 m2.
- Lay-by (LB): No. 19, each at L ≤ 375m distance; Lay-bys will be provided in Escape Tunnel along the length on Right side which will act like truck turning Niche/Over taking zone.

- Cross passages (CP): No. 21, Lmean = 15 m each at L ≤ 375m distance; Vehicular (CPB) and pedestrian (CPA) cross passage will be arranged in order to have alternatively 1 CPB and 2 CPA.
- Adit: No. 1 length = approx. 585 m. Salient geometric characteristics of Adit: (a) the Adit will be located at Chainage Km129.010 (b) Finished Cross sectional Area: 38.2 m2 (c) Mean Cross sectional Area: 57.3 m2.
- Underground electrical substation (Medium Voltage Sub-station Niches): No.3; for E&M safety provisions. USS No.1 will be located in correspondence of LB5; USS No.2 will be located along the Adit1; USS No.3 will be located in correspondence of LB14.

4.3 *The geological and geomechanical context*

The T-74R crosses the rock masses belonging to Ramsu Formation and, in the northernmost sector of the alignment, those referred to Machal Formation. These Formations make part of the so called "Tethyan Zone" representing the metamorphosed sedimentary cover of the High Himalayan crystalline (HHC).

Both Ramsu (pyritiferous slate, carbonaceous shale, crystalline limestone, pebbly phyllite and basic intrusive) and Machal Formations include predominant phillites and slate, but they differ for the higher presence of interlayered quarzites and schists and marbles in the Ramsu formation and for the minor occurrence of quartzite and agglomeratic tuffs in the Machal formation (see Fig. 7 – left). The rocks belonging to the Ramsu and Machal Formation have undergone a complex history of burying and following exhumation, having been subject to huge stresses either in ductile or in fragile conditions (see Fig. 7 – right).

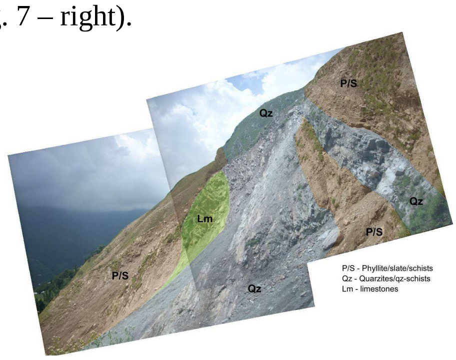

Figure 7 (left) interlayering of mainly quarzites and schists with less yellowish-white limestones at the bottom are visible in the scarp - detachment zone of the active debris flow as well as completely loosened, disjointed and instable, rock mass outcrops on top (right) the main foliation and two cleavages affects this rock mass portion witnessing the long strain history

From the geomorphologic point of view, in the Project area there is a huge and high speed activity of landscape geomorphologic re-modelling.

The different rock masses interested by the project are analyzed considering their overall geo-structural features, as well as their singular components (intact rock, discontinuities). The variability and residual uncertainties on the geotechnical properties are analyzed both with statistical methods and deterministic methods approaches. The resulting characterization is the base of the process of geomechanical classification of rock masses by fabric and quality indexes.

For the geomechanical classification of rock masses different systems are used with specific purpose:

- GSI (Geological Strength Index, Hoek et al.,1995): the GSI is used as a pure fabric index (Tzamos and Sofianos, 2007) to reduce the intact rock properties to the ones of the in situ rock mass, according to the equivalent-continuum approach. The GSI is calculated both by using the original qualitative method (Hoek, 1995) and the new quantitative approach (Russo, 2007,a,b) based on the relationship between GSI and the Joint Parameter (JP) of the RMi system (Palmstrom, 1996), considering that both are used to scale down the intact rock strength σcm to rock mass strength (σc). The following photo and graphic are an example of the structural survey n° M.25.13.3_Above BH5A.

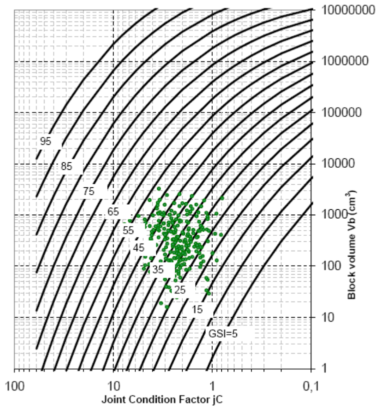

Figure 8 Example of GSI estimation using the quantitative probabilistic approach (Russo, 2007) for structural surveys M.25.13.3_Above BH5A – Statistic analysis of GSI: Min: 13, Average: 35, Max: 57 and Dev.st: 8.

- RMR (Rock Mass Rating, Bieniawski, 1973 and followings). The RMR system is mainly applied for its well-known empirical relationship with the self-supporting capacity of rock masses, as resulting by its geo-structural features, groundwater conditions and orientation of discontinuities. As described in the relevant section, from the combination of stress analysis (→competency) and geo-structural analysis (RMR→stand-up time) the general classification of excavation behaviour is derived and the typical deformation phenomena (hazards) are identified.

The statistical analysis is done for the different lithology intercepted at the tunnel level, taking into account the results coming from each structural surveys (obtained using a probabilistic analysis). The final distribution of the GSI values for each lithology (prevalently phyllites and quartz-phyllites as the predominant litologies), in term of variability frequency, is so graphed as in the following tables. A summary of GSI groups and uniaxial compressive strength (C0) for the different lithology expected along the T-74R tunnel are summarized in the following table.

Table 8 GSI and C0 range values for the different lithologies.

Phyllite		
GSI groups	GSI range	C0 (MPa)
2_GSI	45<GSI<65	50÷100
3_GSI	25<GSI<45	25÷50
4_GSI	GSI<25	<25
Qz - Phyllite		
GSI groups	GSI range	C0 (MPa)
2_GSI	45<GSI<65	50÷150
3_GSI	25<GSi<45	25÷50
4_GSI	GSI<25	<25
Micacoeus Quartzite / Metaconglomerates		
GSI groups	GSI range	C0 (MPa)
1_GSI	GSI>65	50÷150
2_GSI	45<GSI<65	
3_GSI	25<GSI<45	25÷50
4_GSI	GSI<25	<25

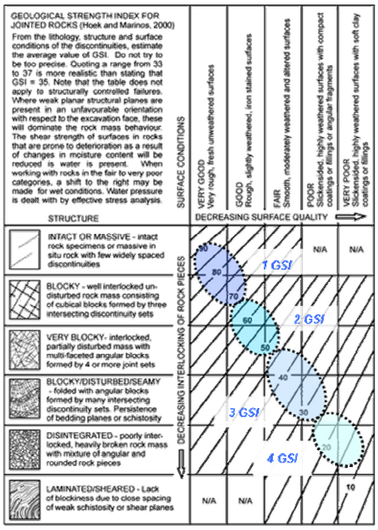

Distribution on Hoek & Marinos's chart (2000) of n°4 GSI groups using for the mechanical characterization of rock masses

4.4 *The selected section types*

The Detailed Design has been developed principally in accordance with the recommendations indicated in “Guidelines for Design, Tendering and Construction of Underground Works” elaborated by SIG (Italian Tunneling Association) in 1997 in relation to tunnelling. These “Guidelines” are based on the identification of the “key points” and their organization into “subjects” representing the various successive aspects of the problem to be analyzed and quantified during design/tendering/construction. The degree of detail of each “key point” depends on the peculiarities of the specific project and design stage. The process involves the following essential phases:

- General setting of the underground work;
- Geological survey and
- Geotechnical-geomechanical studies;
- Prediction of mechanical behaviour of the rock masses;
- Design choices and calculations;
- Design of auxiliary work and tender documents;
- Monitoring during construction and operation.

The mechanical behaviour to excavation has been defined following the graph described in Table 9.

Table 9 - Classification scheme of the excavation behaviour (Russo & Grasso, 2006, 2007, modified).

↓ANALYSIS→		Geostructural→		Rock mass: Continuous ↔ Discontinuous ↔ Equivalent C.				
Tensional↓				RMR				
Deformational response ↓	δ_0 (%)	R_{pl}/R_0	Behavioural category ↓	I	II	III	IV	V
Elastic ($\sigma_\theta<\sigma_{cm}$)	negligible	-	a	STABLE				
			b		INSTABLE			CAVING
Elastic - Plastic ($\sigma_\theta\geq\sigma_{cm}$)	<0.5	1-2	c	SPALLING/ ROCKBURST	WEDGES			
	0.5-1.0	2-4	d					
	>1.0	>4	e				SQUEEZING	
			(f)	→ Immediate collapse of tunnel face ↑				

The main characteristics of the proposed sections for the T-74R main tunnel are shown in the figure 9.

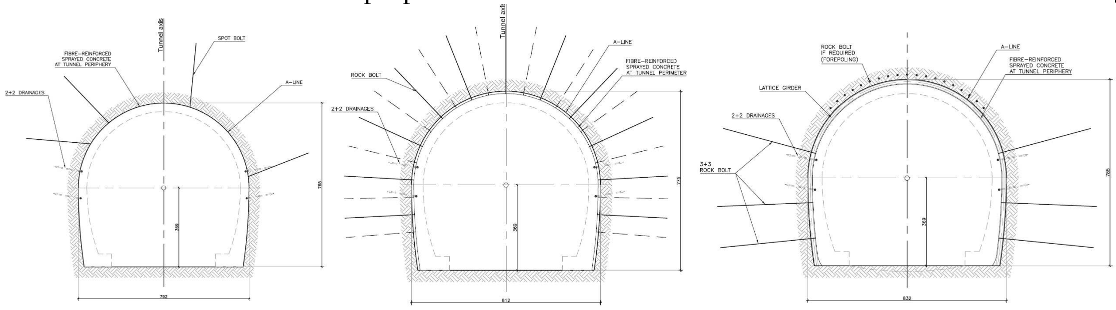

Section type A Section type B Section type C1

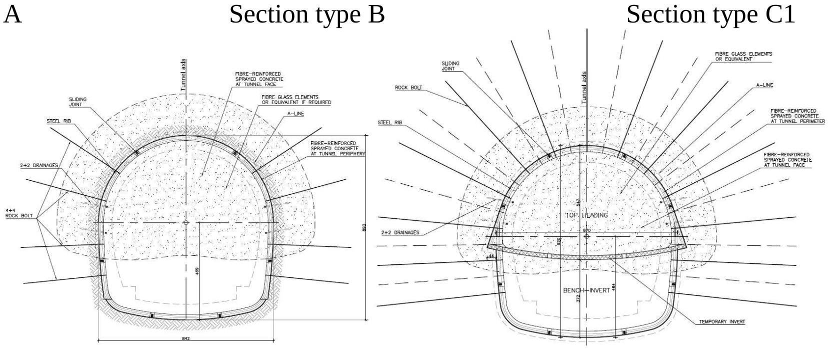

Section type D Section type E

Figure9 Support sections adopted for the Main Tunnel.

The present paragraph will deal particularly with a critical zone represented by intersection between main tunnel and existing T74 tunnel at CH 132+942.01 (Figure 10 and 11).

Figure 10 – Intersection zone between Main tunnel and T74 existing tunnel

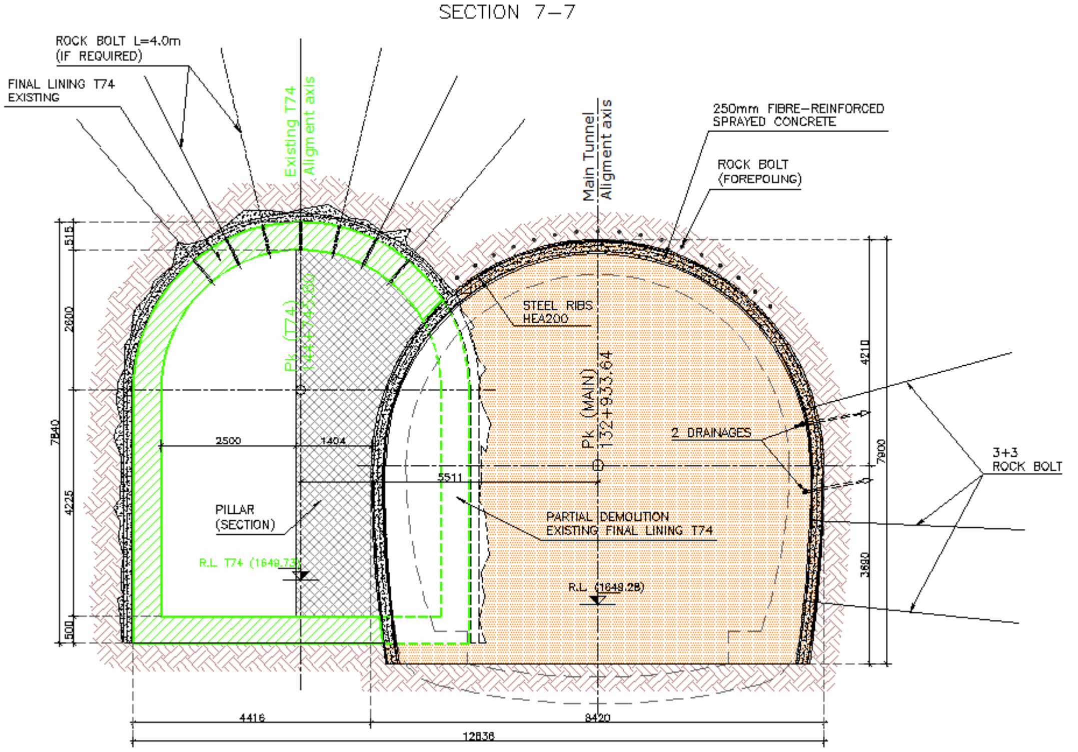

Figure 11 – Cross section of the intersection

4.5 *The seismic input data*

Seismic coefficient to be followed in seismic-based design of T74R tunnel is (Ref :IS 1893 Part1:2002):

$$A_h = \frac{ZIS_a}{2Rg}$$

T74R tunnel falls in seismic zone V as per the Indian Earthquake standard IS1893:2002. The seismic zoning is presented in Figure 12**Figure** :

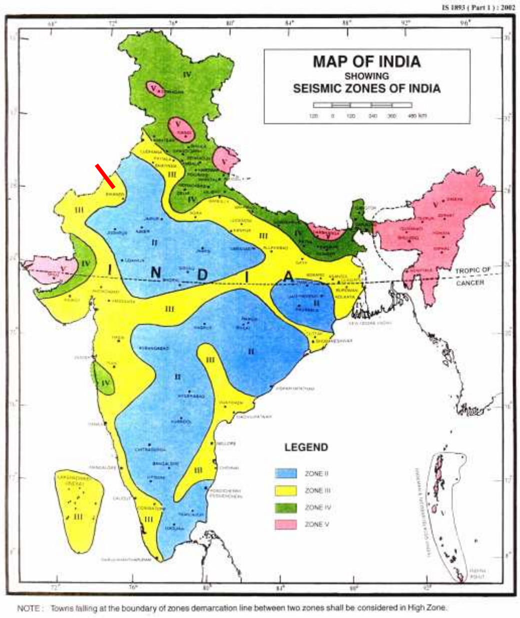

Figure 12 – Seismic zones of India (figure from IS1893:2002)

The zone factor (Z) related to Zone V is 0.36 (Table 2:IS1893:2002).

The importance factor (I) was chosen to be 1.5 to meet the seismic design requirements (Table 6: IS1893:2002). The Response reduction factor is given a minimum value of 1.5.

The average response acceleration coefficient for rock and soil is given Figure 13.

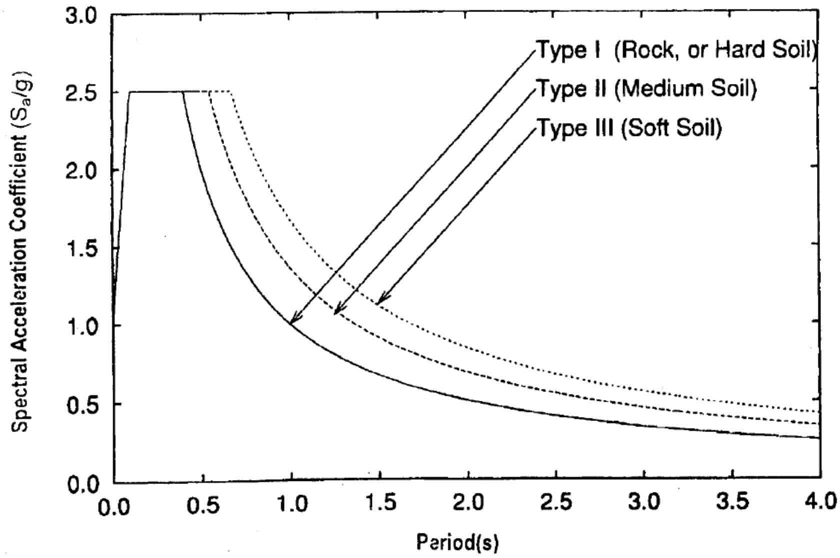

Figure 13 – Response spectra for rock and soil sites for 5% damping

4.6 *Numerical analysis and results*

Numerical model for the application of the Free-Field Shear Deformations Method is shown below:

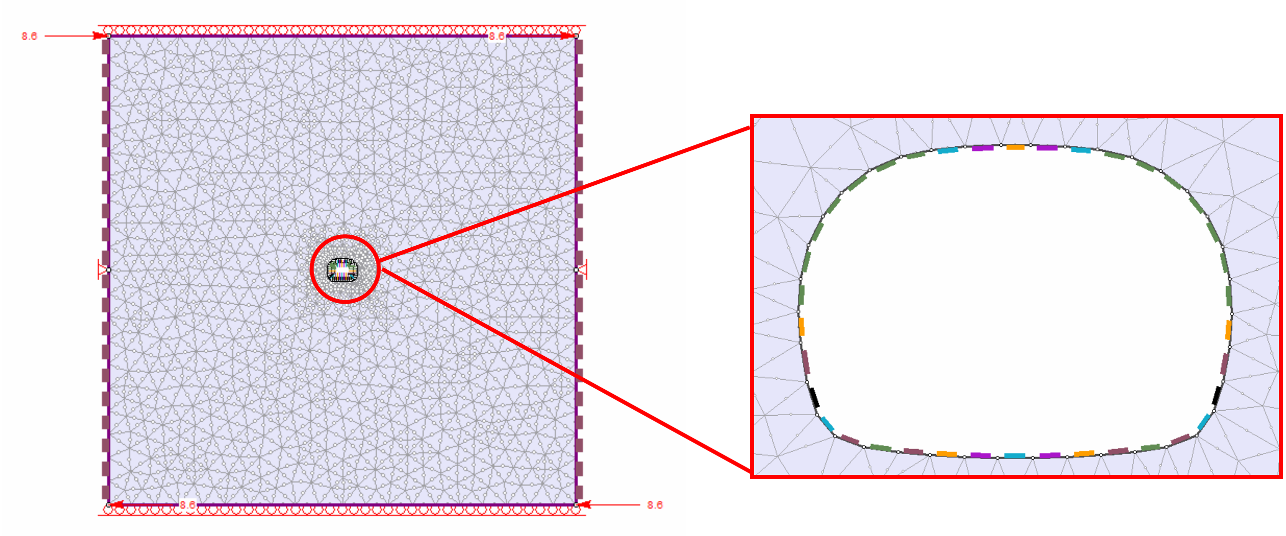

Figure 14 – Section type enlargement 6 - 6. Seismic model

In the next figure, the results of the model are illustrated:

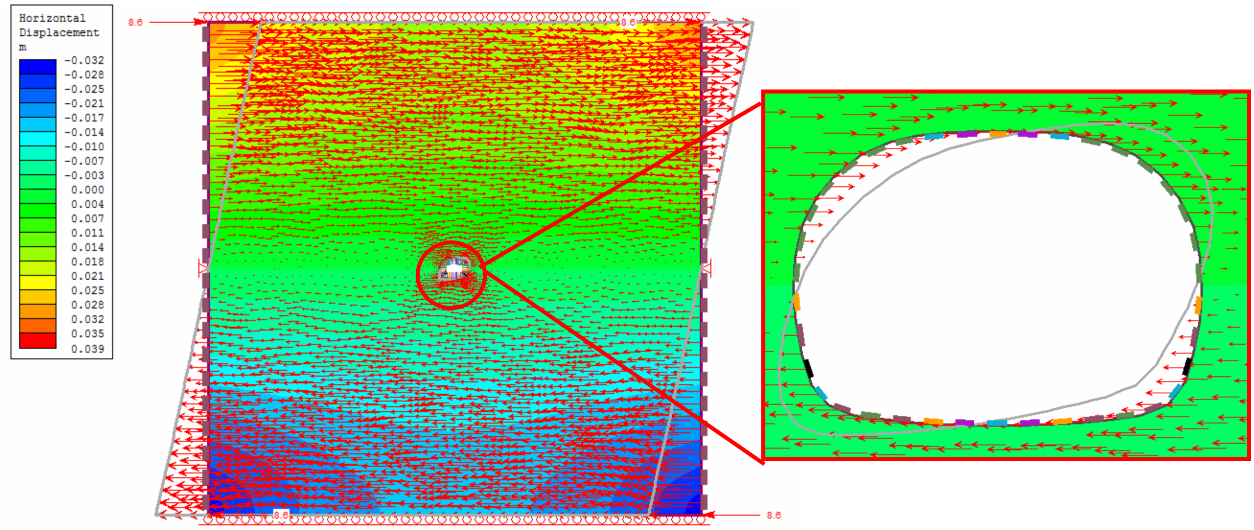

Figure 15 – Section type enlargement 6 - 6. Results of seismic model

In the following tables are reported static (k) and seismic forces (e) obtained from calculation. Static and seismic forces have been combined and a load factor equals to 1.0 have been considered.

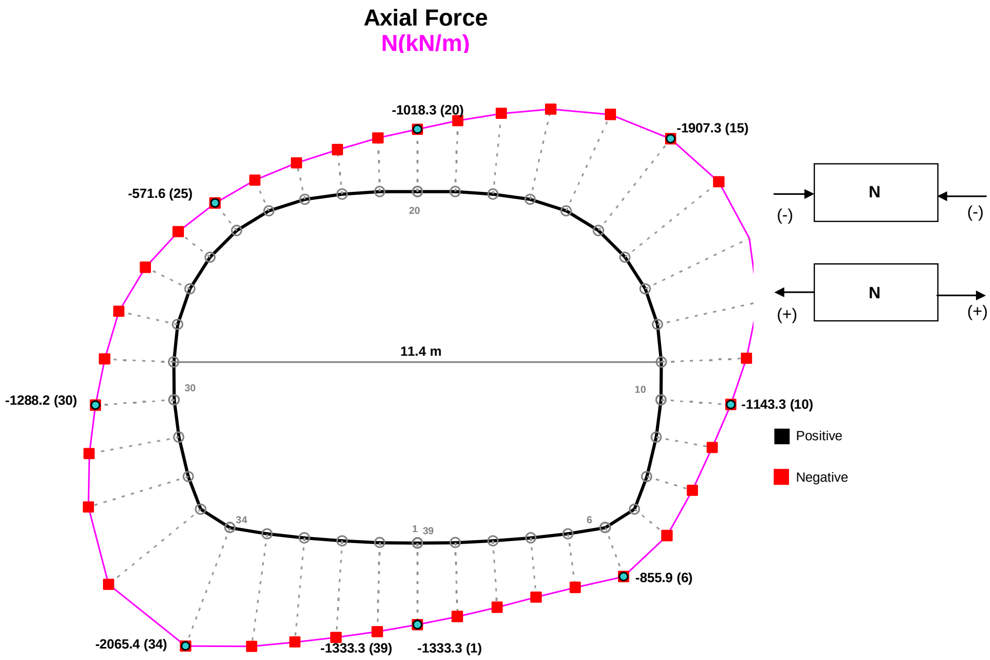

Figure 16 – Section type enlargement 6 - 6. Axial force Ne+k

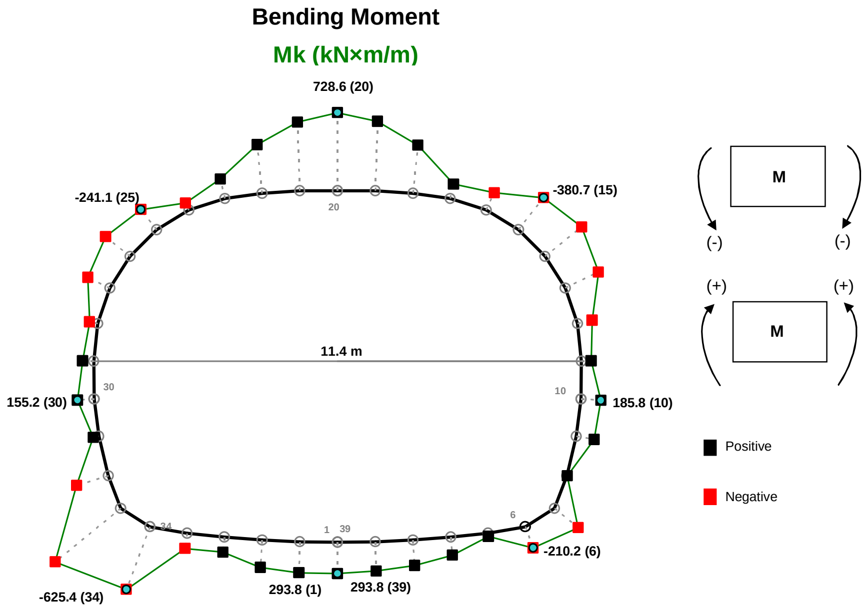

Figure 17 – Section type enlargement 6 - 6. Bending moment Me+k

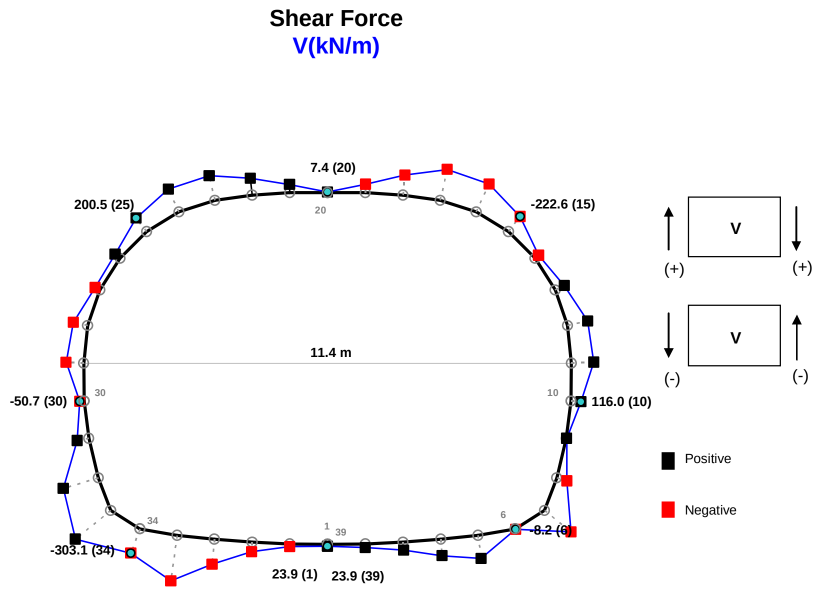

Figure 18 – Section type enlargement 6 - 6. Shear force Ve+k

Next shows the result of ULS verification considering final lining reinforced with 5+5Φ20 as principal steel bars. In correspondence of the crown, 5Φ20 have been added at the intradox of the final lining:

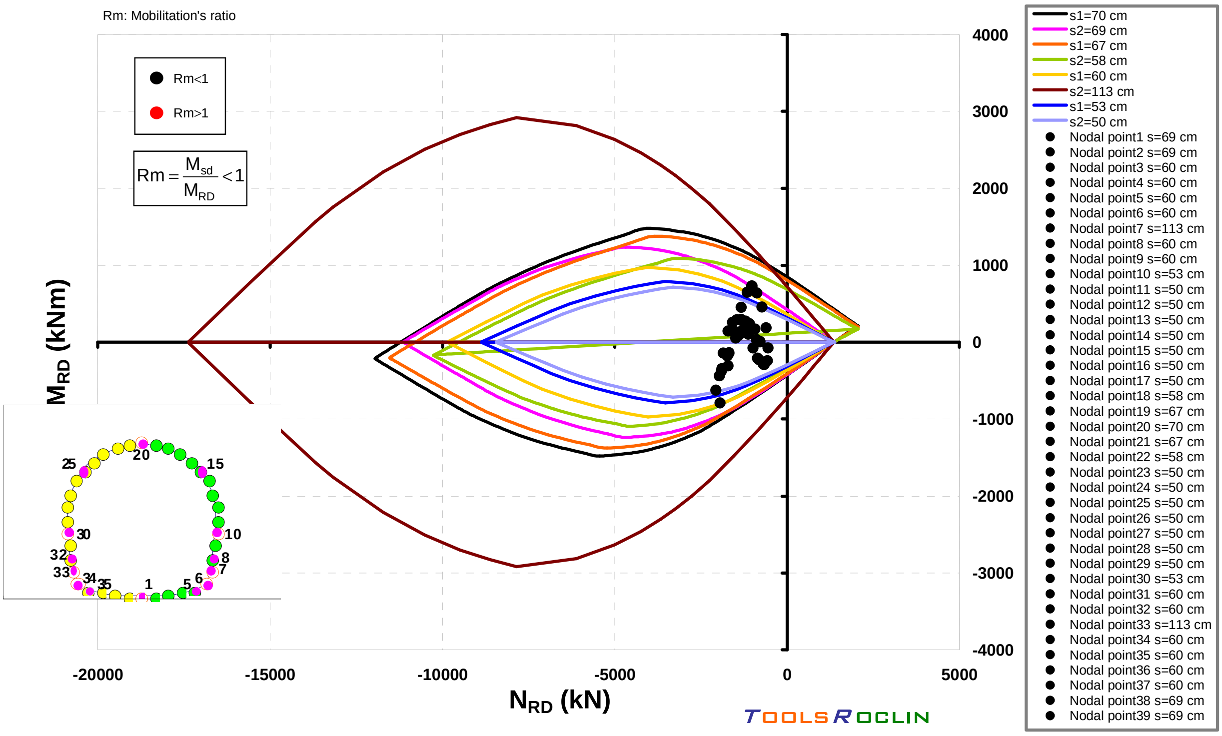

Figure 19 – Section type enlargement 6 - 6. Seismic verification

In the next graph, a comparison between design moment Me+k and resistant moment Mrd is shown:

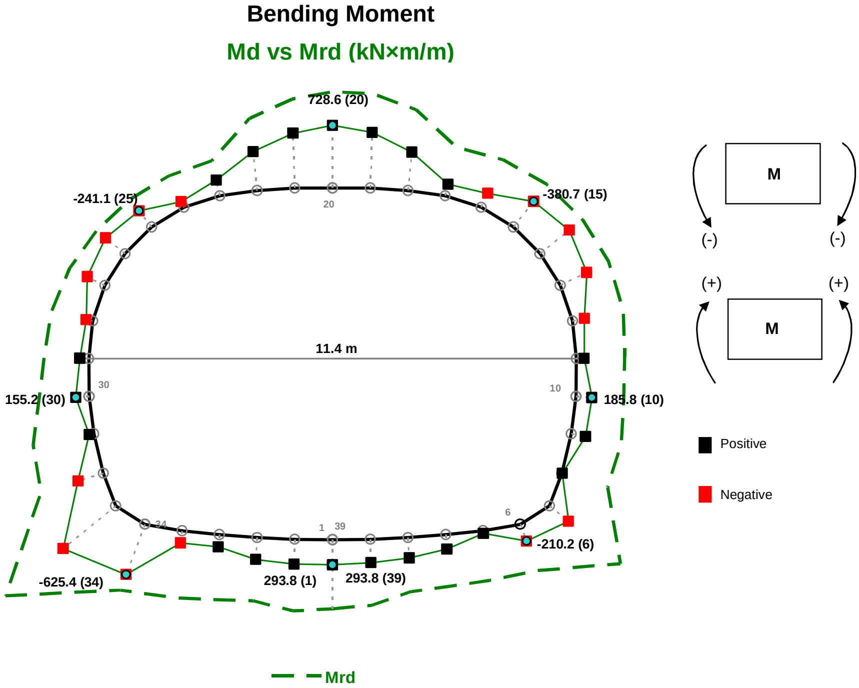

Figure 20 – Section type enlargement 6 - 6. Me+k versus Mrd

5 A METRO TUNNEL THE KADIKOY-KARTAL METRO LINE

5.1 *Istanbul city and Metro line*

Istanbul is a megalopolis with over 13-million inhabitants characterized by a mixture of historic heritage and uncontrolled urbanisation. The biggest problem of the megalopolis is its mobility, owing also to its location, divided in two by the Bosporus, separating the Asian and the Anatolian side (Fig. 21).

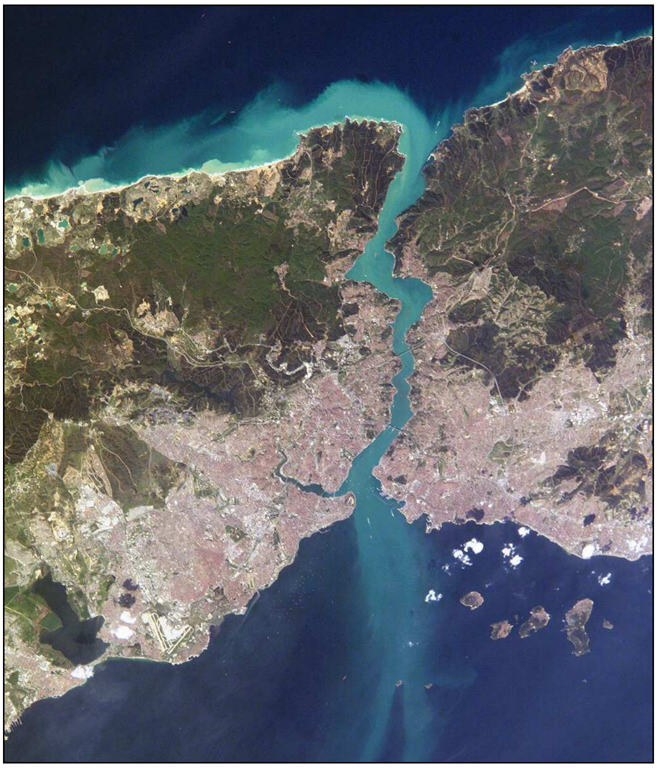

Figure 21. Istanbul city and Bosporus satellite view.

Currently, the only possibility of connecting directly the two parts of the city is to use its two bridges that suffer from high congestion, or, alternatively, to use the various ferry crossings between the two banks of the Bosporus. Nowadays, a development program is activated in order to facilitate the movement between the two sides. In this context the Kadikoy-Kartal metro line will be the new backbone of Istanbul's public mass transport system in the Anatolian side of the city (Fig. 22).

Figure 22. Istanbul city plan view.

The line mainly runs beneath the E-5/D100 corridor, the main urban highway linking the two parts of the city. The line is designed to be completely underground, with a cover varying between 25 and 35m. As a result, all works, including the platform tunnels of the stations, have been conceived as deep underground excavations in order to limit the impact to the surface, including the construction of shafts to access the excavation fronts.

The length of the line, including also the extension, is approximately 26km, consisting of two single-track tunnels with 19 stations. Considering the tight time schedule imposed by the Municipality, the excavation planning foresaw three main stretches realized by different methodologies and contractors (AVMG – Avrasya Metro Grubu – and Anadoluray):

- Stretch 1: Kadikoy – Kozyatagi: 9km long (excavation technique: Tunnel Boring Machine (TBM) – by Anadoluray);
- Stretch 2: Kozyatagi – Kartal: 13km long (excavation technique: mined tunnels – by AVMG);
- Stretch 3: Kartal – Kaynarca: 4.5km long (excavation technique: TBM – by AVMG).

The stations are constructed with the cut & cover technique, except for the Acibadem and Bostanci stations that are being excavated as mined station due to interference problems; the platforms, connection tunnels and switch tunnels are executed by conventional tunnelling techniques; along the entire line these structures have to be realized by AVMG. The running tunnels are excavated both by TBM (approximately 13.5km by two different contractors, AVMG and Anadoluray) and by conventional method (approximately 13km by AVMG).

GEODATA has been in charge of the design of all conventional tunnelling works to be executed by AVMG (access shaft, running tunnels, platform tunnels, switch tunnels and connections).

5.2 *Tunnelling works*

The line consists of two single-track running tunnels and involves the construction of several complex safety cross passages and train switches. The latter works, when combined with the station-platform tunnels, form practically large caverns whose cross sectional area can reach up to 175m^2. In detail, the typical layout of the underground works, to be excavated with conventional methods, is characterized by the following main typologies:

- Switch tunnels: including the excavation of one or more shafts, the shaft-access tunnel and the switch tunnels themselves;
- Stations: including platform tunnels, connection tunnels, stairs tunnels, ventilation tunnels, ventilation shafts and other underground spaces required.

According to the design criteria, all these underground spaces constructed by conventional method should be completed before the passage of TBMs. In addition, in some points of the alignment, a number of further underground spaces are required, such as the Kartal node which will be the launching spot of the TBMs; here a big cavern has been excavated with a sectional area of more than 200m^2.

The needed internal dimensions of the various tunnels must be taken into account in the design process of the project. Alternatively, depending on the design criteria and the engineering decision taken for each situation, the external diameters can be defined so as to meet the project requirements. This has led to a complex condition where more than 15 geometrical typical sections are to be provided. Some examples of these typical sections are shown in Fig. 23 while Fig. 24 illustrates schematically the three-dimensional complexity of a typical station with the various underground spaces mentioned above. In particular, in this paper the switch M1-M4 final structures design will be described as example of seismic resistant design with the proposed simplified approach.

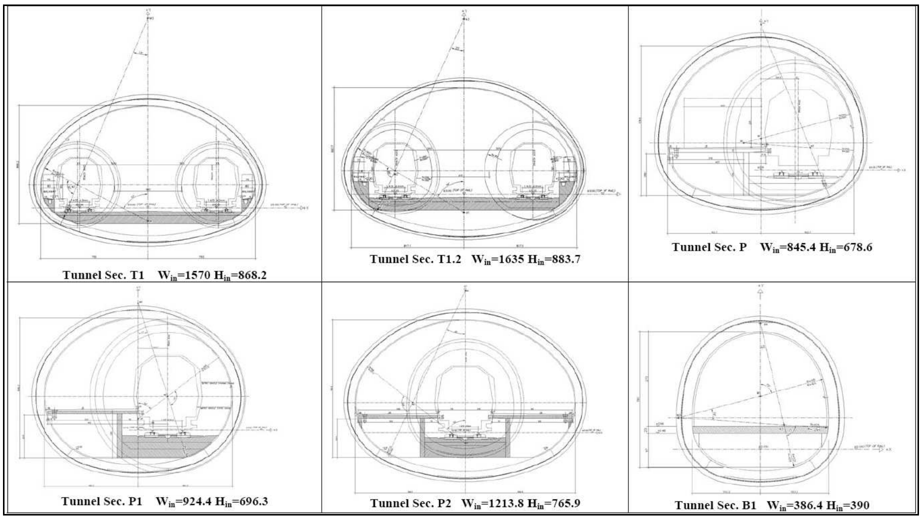

Figure 23. Typical sections for switches and platform tunnels

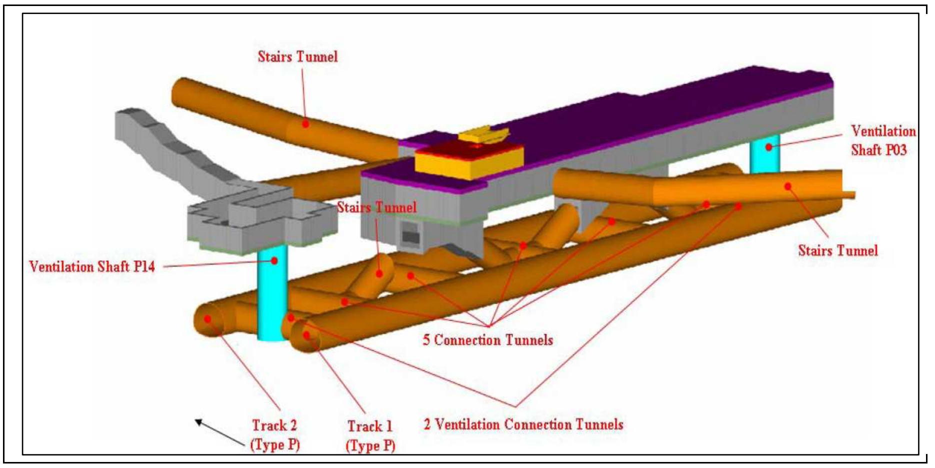

Figure 24 Typical 3D layout of stations.

5.3 *Geological context*

The Istanbul region is characterized by a well developed, unmetamorphosed and little deformed continuous Palaeozoic sedimentary succession. The initial part of the alignment (Kadikoy side), crosses first the Trakya formation, then runs in a transition in the Kartal and Kurtkoy formations, followed by the Dolayoba formation (Fig. 25): thus the geology of Switch M1-M4 is very variable, mainly characterized by siltstone, sandstone and claystone The alignment also passes through various magmatic intrusions and fault zones, which could be expected even in the first stretch, close to this Switch.

The geological context of the Kadikoy-Kartal alignment is composed of six main geological formations: they have been encountered by the underground works with rock types ranging from sedimentary to volcanic rock type. The rock masses are characterized by high variability of the weathering condition, from slightly weathered (W1) to completely weathered (W5) down to residual soil, as confirmed during the excavation works.

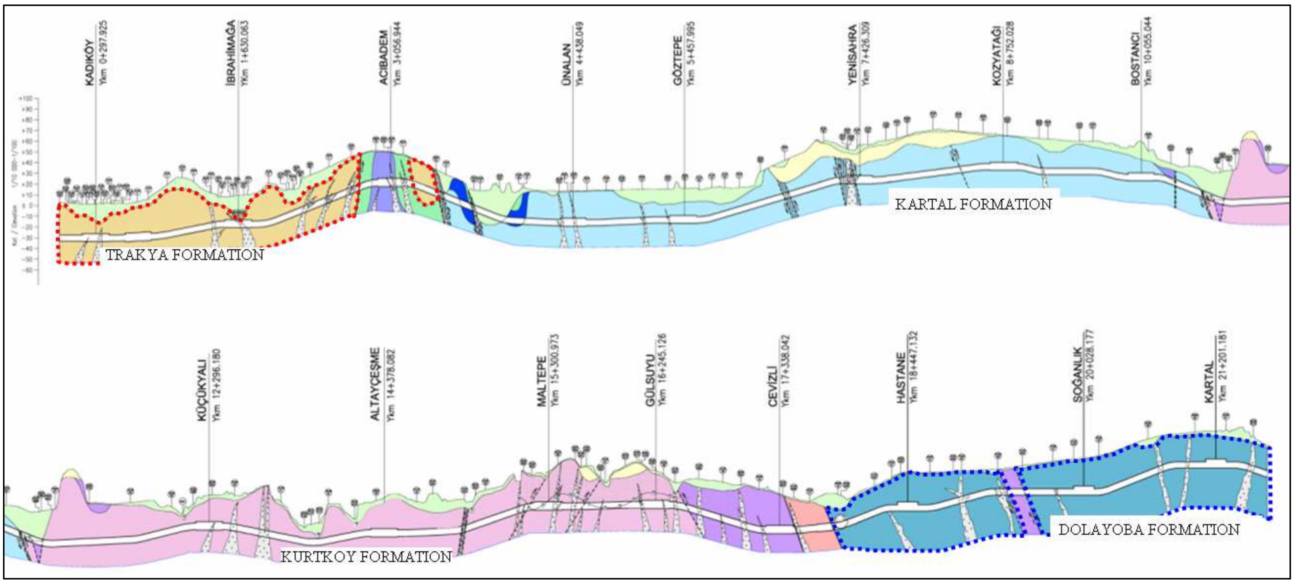

Figure 25. Longitudinal geological profile and evidence of the Trakya formation which characterizes Switch M1-M4.

Groundwater presents another critical issue for some areas such as Kadikoy, where the station and switch tunnels are located in the close vicinity of Marmara Sea, with the rail level being at approximately 30m below the sea level. All underground structures in the Metro alignment are designed to be full-round waterproofed. Furthermore, in Kadikoy area specific materials have to be used according with the used Standard codes [Eurocodes and Turkish codes], as previously reported; for example, the concrete used to realize the final structures of Kadikoy switch and stations (including both the underground and cut & cover structures) was characterised by a C35/45 grade and an exposure class XS2 (so that to avoid potential steel corrosion induced by the chlorides from sea water).

5.4 *Kadikoy-Kartal Metro Line: Design Earthquake Ground Motions*

Due to the high seismicity level of Istanbul (Fig. 26), it is a requirement of the Municipality that all the final linings have to be designed to resist the seismic loads. However, the risk of having seismic event during the construction period of about 4 years was not considered in the design of the temporary support.

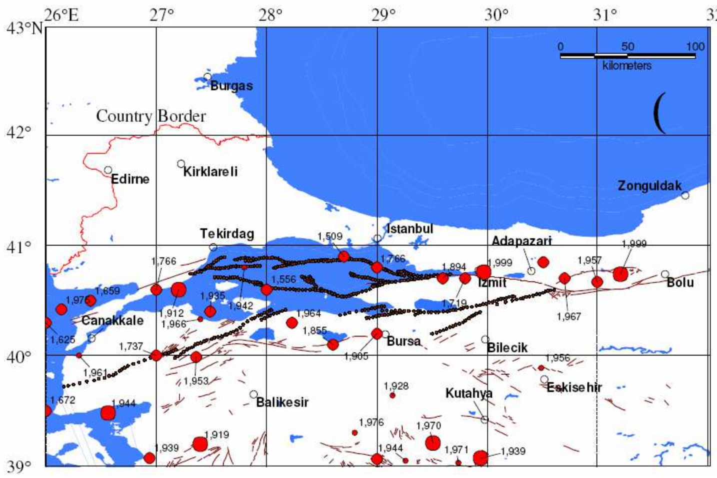

Figure 26 . Historical and instrumental seismicity of the “Straits Region” and tectonic faults [Ambraseys and Finkel, 1991].

For the seismic design of the Kadikoy-Kartal Mass Transportation Route two levels of ground motion are considered for earthquake resistance design purposes:

Functional Evaluation Earthquake Ground Motion (S1):

This ground motion refers to earthquakes that can reasonably affect the transportation route at any location during its lifetime. Considering the seismicity of the region and the importance of the tunnels, it will be prudent to assign a 50% probability of exceedance in 50 years. This ground motion level will also be checked with a deterministic median (50 percentile) that would result from a Mw=7.5 scenario earthquake occurring on the Main Marmara Fault: the larger of the two assessments will be selected.

Under exposure to this ground motion the transportation system will be fully operational (essentially linearly elastic performance).

Safety Evaluation Earthquake Ground Motion (S2):

This ground motion can be assessed either deterministically or probabilistically. The probabilistic ground motion for the safety evaluation typically has a long return period (approximately 2500 years), which corresponds to 2% probability of exceedance during 50 years. This level of ground motion is associated with the Maximum Credible Earthquake (MCE) is defined as the largest earthquake, that is capable of occurring along an earthquake fault, based on current geologic information, which is quite similar, if not identical to the NEHRP (2003) definition.

The AGI Guidelines for geotechnical aspects of seismic design also mention (Silvestri and Simonelli, 2005) two levels (L1 and L2) for the definition of the design earthquake ground motions, respectively for probability of exceedence of 50% and 10% of the reference lifetime (differently than the Italian Code NTC 2008, which defines four levels). The cited Authors assume a probability of 2% rather than 10% for MCE: this choice is as well consistent with NEHRP (2003) indications which consider that the use of 10% may be not sufficiently conservative in the central and eastern United States where the earthquakes are expected to occur infrequently compared to California.

In practice, this choice considers that the ground motion difference between the 10 percent probability of exceedance and the 2 percent probability of exceedance in 50 years is typically smaller in coastal California than in less active seismic areas (such as the eastern or central United States). The same choice appeared adequate for the Marmara Region in Turkey, as the experimented damages due to seismic actions on tunnels in the last few years were really elevate: as instance, the Bolu Tunnels during the 1999 Duzce earthquake [Case stuffy on seismic tunnel response, Kontoe, Zdravkovic, Potts and Menkiti, Canadian Geotechinical Journal 45:1743-1764, 2008].

For the verifications, it must be considered that under Safety Evaluation Earthquake only repairable damage with no danger to life is allowed.

5.5 *Expected performance levels under design ground motions*

The performance levels expected under S1 and S2 ground motions are defined below:

Earthquake Level	Expected Performance	
	Functionality	*Damage*
S1	Continuous	Minimal
S2	Limited	Considerable but still repairable

"Continuous Functionality" performance criterion refers to the uninterrupted service of the structure immediately after an earthquake. On the other hand the "Limited Functionality" performance criterion will guarantee only limited use a few days after an earthquake. Full functionality is aimed to be obtained in at least a few months. The "Minimal" damage criterion refers to the nearly linearly-elastic response. To meet the performance criteria required under the S1 earthquake the "Response Modification Factor" (damping factor of the structures) should not exceed 2 [Caltrans, 1999]. The "Repairable" Damages should be repaired with minimum effects on functionality. The "Considerable" damages should not cause total collapse and loss of life.

These S1 and S2 levels of ground motion were originally quantified in frequency domain using the standardized response spectral shape of NEHRP, 2003 or IBC, 2006 in terms of the short-period (0.2s) and 1s-period spectral amplitudes at NEHRP B/C site class boundary. The site dependent spectra was then generated using the NEHRP Site Class definitions and the associated spectral site amplification factors [Erdik et al., 2008].

The standard shape of the response spectrum was taken equal to the so-called "Uniform Hazard Response Spectrum" provided in IBC (2006) and NEHRP (2003) Provisions. This spectrum is approximated with the site-specific short-period (S_S) and medium-period (S_1) spectral accelerations as illustrated in Fig. 27.

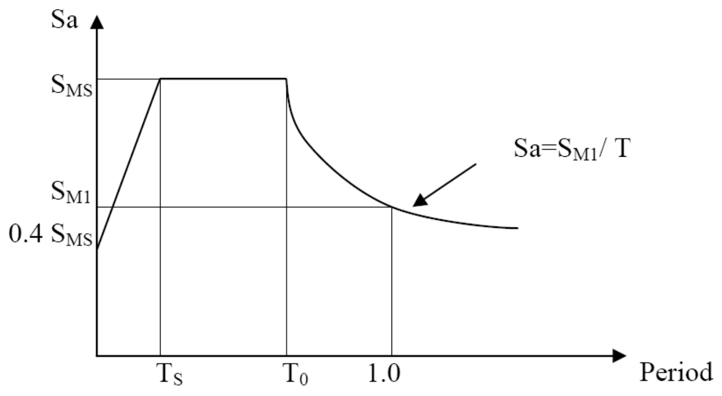

Figure 27. The design response spectrum

Based on the characteristic type earthquake occurrences on the North Anatolian Fault and conditional earthquake probabilities, time dependent probabilistic seismic hazard assessment results (assuming non-poissonian model) have been used for the determination of the seismic hazard. The methodology used in the hazard assessment is essentially taken from the earthquake hazard assessment study conducted for Marmara region [Erdik et al., 2008].

Site dependent Spectral Accelerations (T=0.2 sec and 1.0 sec, S_S and S_1 respectively) with 50% and 2% probabilities of exceedance in 50 years were evaluated for the whole area and an example of those charts is presented in Fig. 28.

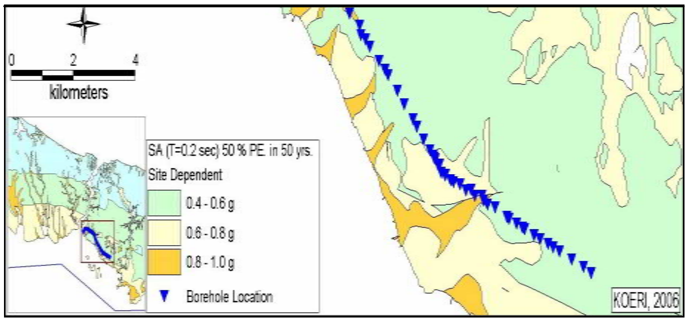

Figure 28. Site dependent Spectral Accelerations (T=0.2 sec, Ss) with 50% probability of exceedance in 50 years [Koeri, 2006].

5.6 *The case-study: Kadikoy switch (M1-M4)*

The case study is a complex underground structure, lying just parallel to the sea side on the Anatolian part of Istanbul. The cave host the connection of the first station of Kadikoy-Kartal metro line to the running tunnels: a switch on the rail is required in order to allow coaches to invert drive direction, thus requiring a huge "gabarit" and consequently a wider cross section than the one of the standard line. Furthermore, its geometry is irregular, characterized by a polycentric edge, with a span of about 17,5 meters and a total maximum height of about 12 meters: the invert thickness, after the dimensioning, was optimized to reach a maximum thickness of less than 160 centimetres.

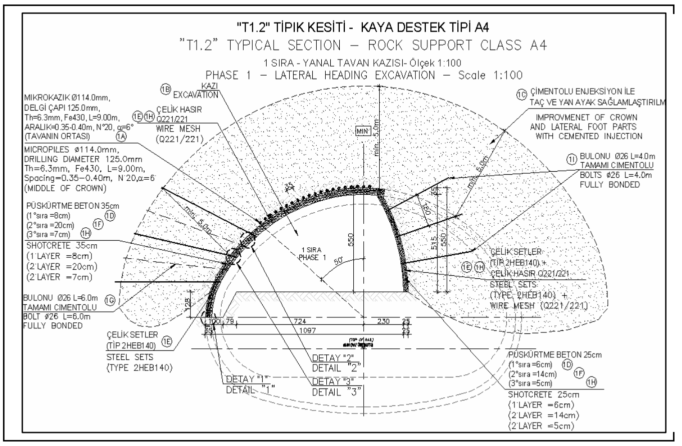

Figure 29. Rock support class adopted for Kadikoy switch.

Figure 30. Kadikoy switch underground structures – completed excavation.

5.7 *Geological features and geomechanical properties*

The Switch M1-M4 is located between kilometres 0+442.373km and 0+604.833km, where the main rock medium is the so-called Trakya Formation. This formation is found under the superficial alluvium layers.

The Trakya formation stands for Greenish gray colour, brown in weathered zone, local lenticular gravel and sandstone stratum formation named by Kaya in 1978. It is generally comprised by shales with tiny layer and parallel lamination. In this shales at various stratigraphical levels there exist yellowish brown sandstone, gravelly sandstone and lenticular gravel formations. The thickness of sandstones varies between 10 cm and 250 cm. Bottom surfaces of these are sharp, weathered and above these levels fossils and base structures with type of flames are seen. These properties evidence that intermediate sandstone layers were settled down by turbid flows. In the piling above, thickness and number of sandstone intermediate layers increases. Besides, at the top section various levels of lenticular gravels exist. The general outlook of Trakya formation is represented in Fig. 31.

Figure 31. : Left: the outcrop of the Trakya formation- view at the Mostra Middle - thick Layered Sandstone. Right: Trakya formation viewed at the face of the access tunnel of shaft S1D.

According to the information of geological and geomechanical reports and profiles, the alluvium soils and fills (clay, sand, gravel, fill) can also be found in Trakya formation as a sub-formation (near surface material). In addition, the magmatic rocks (andesite –diabase) are also found place to place along the alignment in Trakya formation.

Figure 32 illustrates the longitudinal profile of the geological formations over switch tunnel M1-M4. According to the borehole logging data and to core boxes little recovering ratio, a quite poor ground condition is expected as its geomechanical characteristics are highlighted in Table 7. The value of cohesion for Trakya formation was derived from the statistical analysis of logging the boreholes KKS17B,KKS1,KKS1A,KKS18, while the value of cohesion was obtained from empirical equation of Hoek et al. (2002) for tunnel applications.

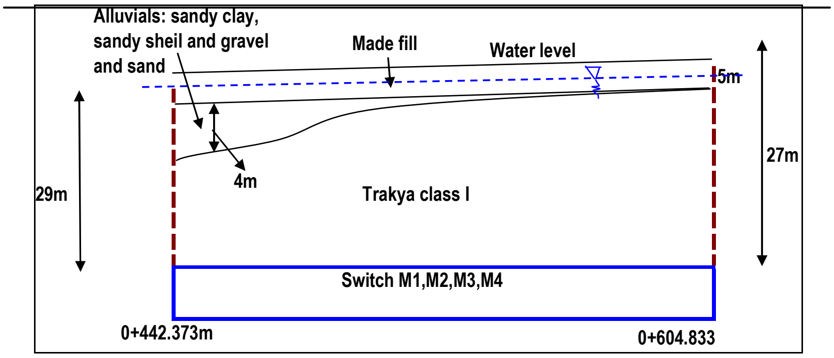

Figure 32: Representation of the longitudinal model for the M1-M4 switch with over-lying geological formations.

Parameters	***Unit weight γ [kN/m3]***	***cohesion c [MPa]***	***Friction angle Φ [°]***	***Poisson's ratio v***	***Deformation Modulus E [MPa]***
Trakya class I	25	0.135	32	0.3	300
Alluvial fill	20	0	26	0.3	25
Made fill	19	0	23	0.35	15

Table 7. Geomechanical characteristics of the ground layers in which the switch M1-M4 was excavated and built.

5.8 *Results of the analyses and dimensioning*

In the case of Switch M1-M4 final structures, a seismic resistant design was performed, giving to the structures the necessary safety requirements as per Eurocodes'. Referring to the methodology above illustrated, the data characterizing the seismic design are reported in Table 8.

Earthquake Level	S_S (g)	a_{gr} (g)	$a_{max,s}$ (g)	a_z (g)	*Vs* (m/s)	*Cs* (m/s)	γ_{max}	Δx_{max} (m)
S1	0.696	0.278	0.278	0.223	0.216	2000	0.000108	0.0075
S2	1.434	0.574	0.574	0.459	0.4451	2000	0.000222	0.0156

Table 8 Summary of the results obtained from seismic analysis method as for the input data of the numerical model.

Numerical analyses (Fig. 33) were carried out in order to find the stresses acting in M1-M4 final lining according with the seismic design. Fig. 34 shows the three parts in which the lining can be divided, in order to be consistent with the homogeneity of thickness (Fig. 35) and/or of stress patterns:

- Crown
- Sidewalls
- Invert

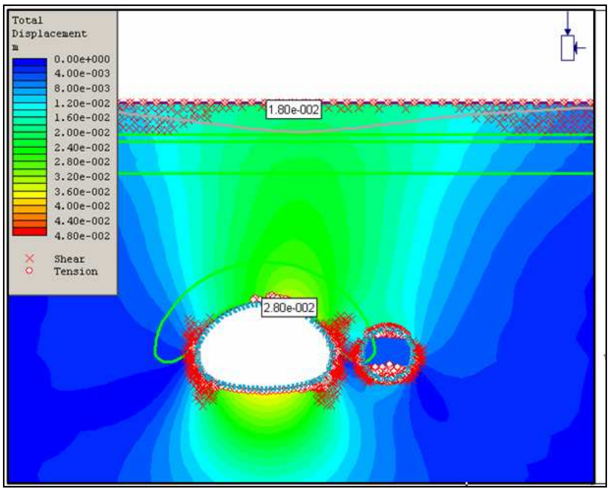

Figure 33. Kadikoy switch revised design

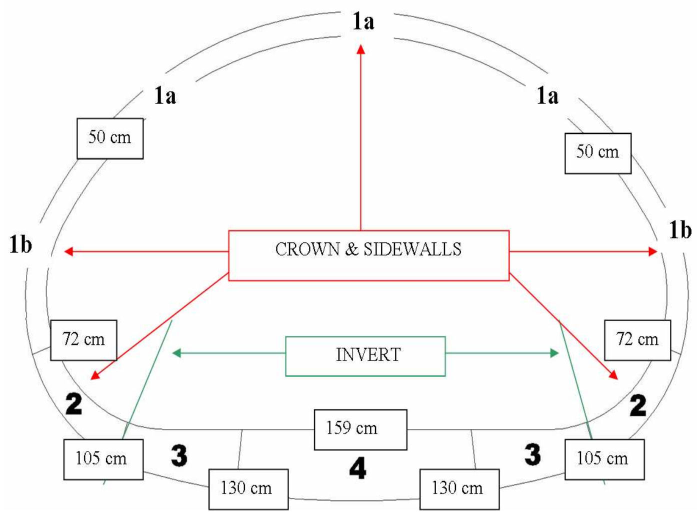

Figure 34. Identification of the main areas of the lining as for an homogeneous distribution of steel reinforcement

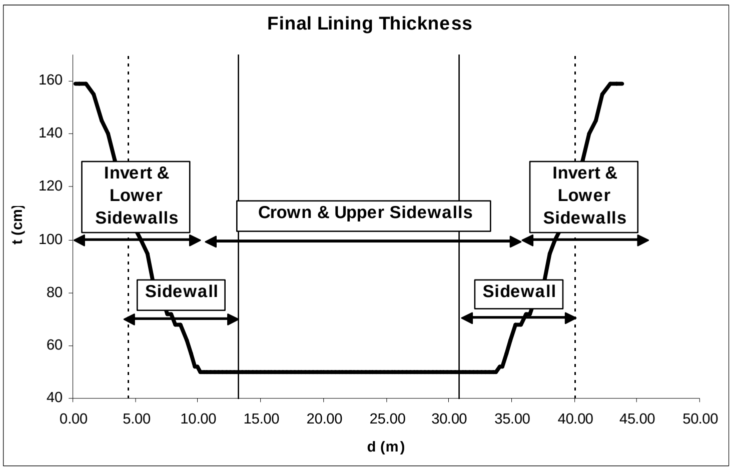

Figure 35. Thickness of the Final Lining.

In the subsequent figures the results of the numerical analyses are shown. In details, Fig. 36 represents axial force (N) - positive values correspond to compressive forces -, bending moment (M) and shear forces (V) in the final lining for the two seismic cases: S1 and S2. It can be noticed how the effects of an earthquake of larger time of occurrence can be almost double in terms of forces and moments. This result was expected from a (pseudo)-static application of an almost double distortion to a linear elastic system. In the reality, the dynamic behaviour of an elastic-visco-plastic system may be different [Amorosi and Boldini, 2009, "Numerical modelling of the transverse dynamic behaviour of circular tunnels in clayey soils", Soil Dynamics and Earthquake Engineering].

The earthquake level S2 in some other cases, when its effects are superposed to the static analyses results (without groundwater presence), gives some tensile force in correspondence of the upper part of the sidewalls, thus specific reinforcements is prescribed in these zones of the structures. Figs. 37 and 38 show, as an instance, the combination between the results of static analysis without water presence and the ones of the seismic numerical modeling for cases S1 and S2 as for Normal Forces, Bending Moments and Shear Forces.

All the load combinations (static and seismic, with and without water load) were verified and the reinforced concrete was dimensioned according with the prescription given by Eurocodes and Turkish Standards. Moreover, the proximity of the sea determines a water table which is very salty and leads to the need of special verification and, as for Eurocode 2 requirements, the use of concrete class higher than everywhere else (R_{ck} 45).

Figures 39, 40 and 41, to conclude, only present an example of the ULS verification of the final lining along the crown, the sidewalls and the invert, joining together in the same graph different beams in which the lining is modelled depending on their thickness. Fig. 34 shows the areas which are homogeneous as for the lining thickness in order to gather together in same graphs the different verifications of crown (Fig.39) and sidewalls (Fig. 40). As for the invert, otherwise, the different thickness at each position of this structure brings to the need of verifying one by one all the different beams, as clearly shown in Fig. 41.

Besides, according to the contents of the article, in those figures there is only the “axial-force/bending moment” verifications carried out for the load combination shown in Figs. 37 and 38, in both the seismic cases S1 and S2. As for the “shear verification”, instead, the maximum shear force between the static and seismic conditions had been verified in each section of the final lining. From the result of structural analyses it’s possible to define the quantity of reinforcing steel for the concrete sections of the final lining (as showed in previous chapter).

The results of the numerical analyses confirmed the adequacy of concrete and steel characteristics. The maximum stresses and deformation of the final lining are acceptable in each section of this switch and as per figures and values above presented the final lining was verified.

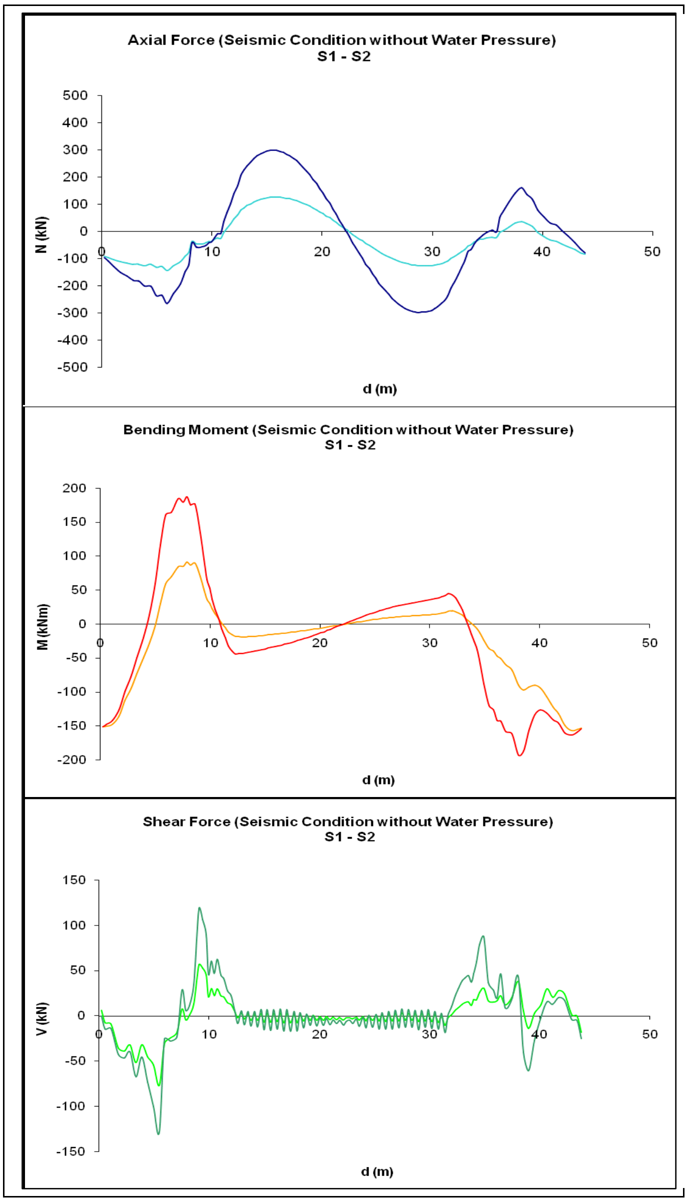

Figure 36. Seismic results as for Normal Forces, Bending Moments and Shear Forces respectively from top to bottom – comparison between S1 and S2 seismic events.

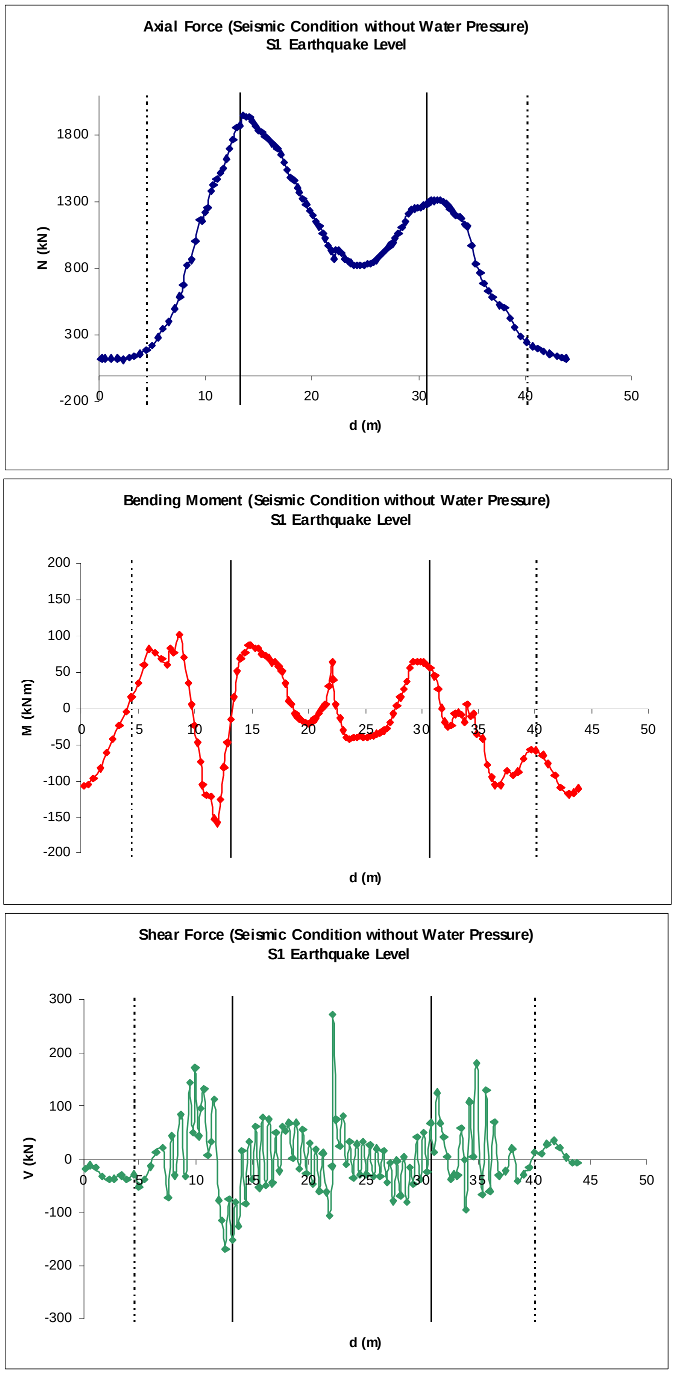

Figure 37. Combination between results as from static analysis without water presence and seismic numerical modeling for case S2 as for Normal Forces, Bending Moments and Shear Forces respectively from top to bottom.

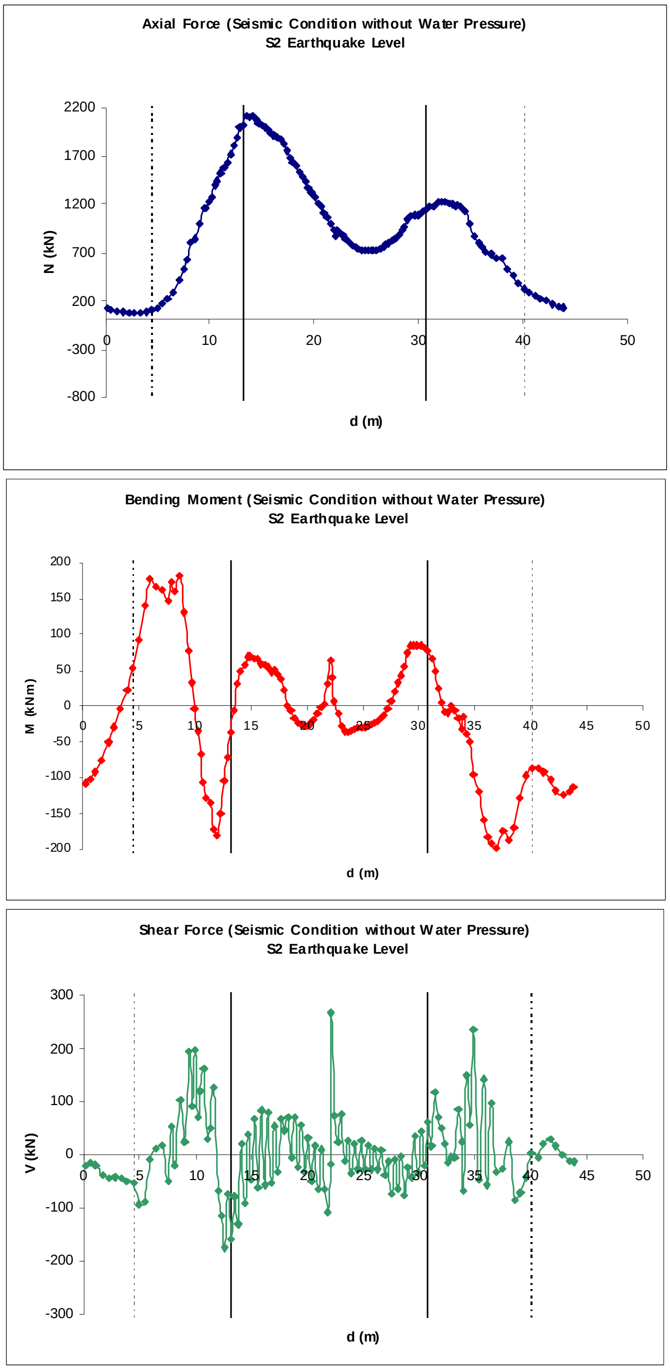

Figure 38. Combination between results as from static analysis without water presence and seismic numerical modeling for case S2 as for Normal Forces, Bending Moments and Shear Forces respectively from top to bottom.

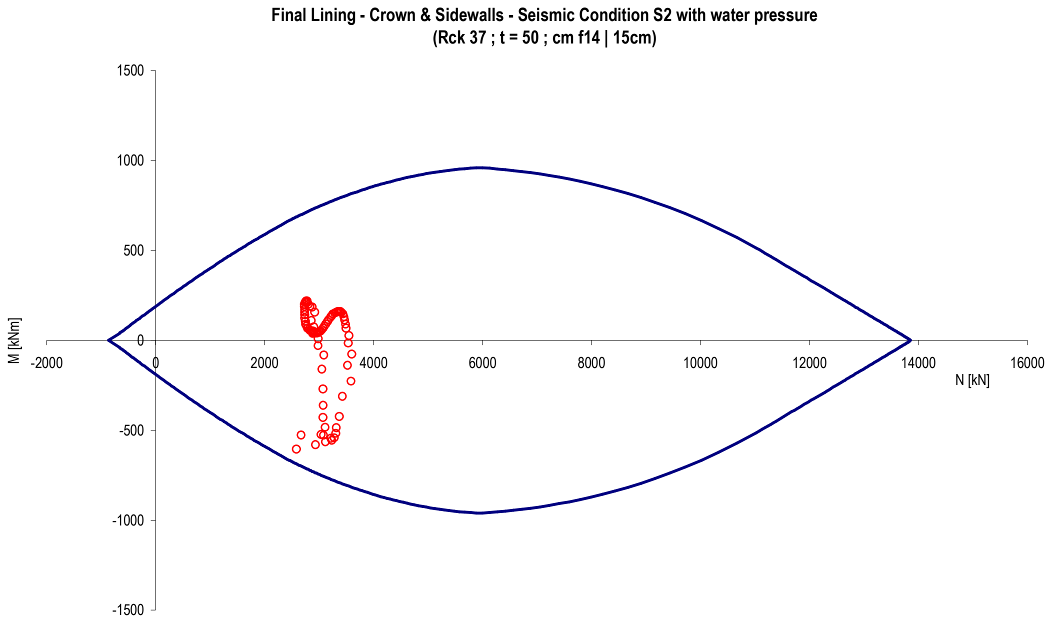

Figure 39. Seismic condition B+C_S2 – Crown and upper sidewalls – Bending moment / Axial force verification.

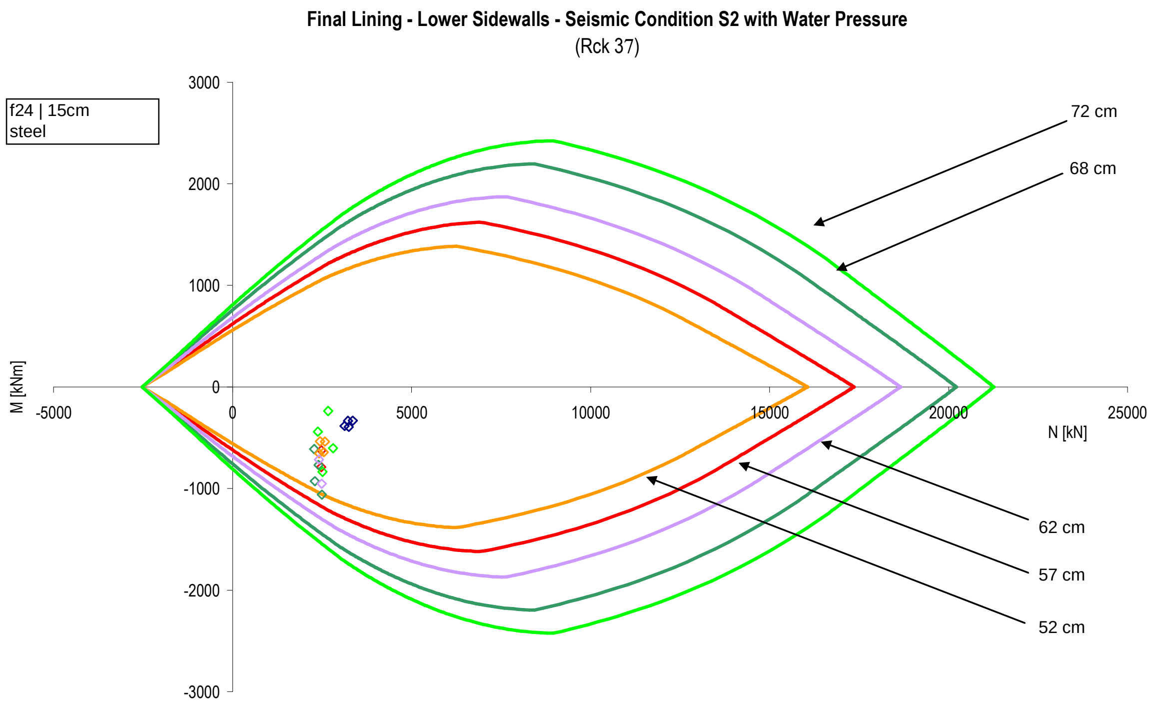

Figure 40. Seismic condition B+C_S2 – Lower sidewalls – Bending moment / Axial force verification.

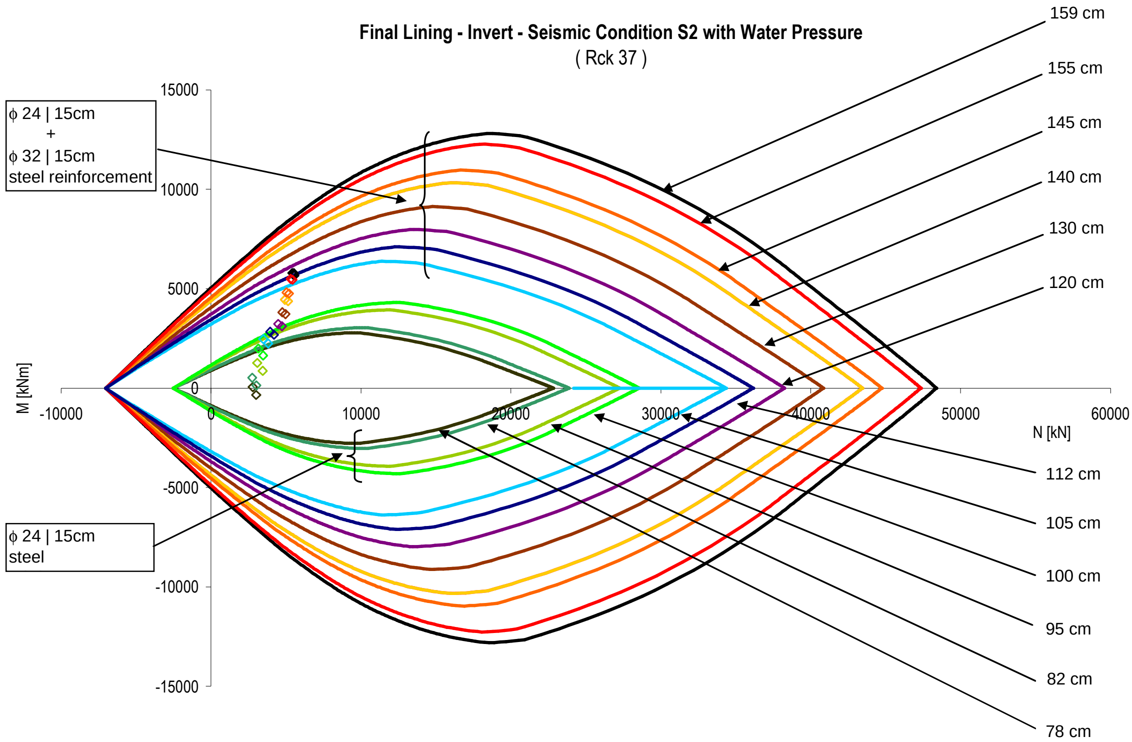

Figure 41. Seismic condition B+C_S2 – Invert – Bending moment / Axial force verification.

6 CONCLUSIONS

The paper has the aim to present a suitable and quick method to perform seismic analysis and verification for some cases of underground structure both in urban area and for long and deep tunnel.
The verification are always possible by common numerical analysis which can take into account the real geometry and the distribution of the surrounding ground.
By a simple superimposition of the effect is also possible to distinguish the static part of the acting force and the seismic components which allow to have a better understanding of the problem.

REFERENCES

AMOROSI A. & BOLDINI D. (2009) - *Numerical modelling of the transverse dynamic behaviour of circular tunnels in clayey soils*, Soil Dynamics and Earthquake Engineering, Volume 29,6 June, pagg. 1059-1072, Elsevier.

AASHTO (1996) - *Standard Specifications for Highway Bridges*. Sixteenth Edition, adopted and published by the American Association of State Highway and Transportation Officials, Washington, DC.

AMBRASEYS N. N. and FINKEL C. F. (1991) - *Long-term seismicity of Istanbul and of the Marmara Sea region*. Terra Nova, III, 527-539.

ATC 32 (2000) - *Improved Seismic Design Criteria for California Bridges: Resource Document*. Applied Technology Council, Report No. XXXII.

AVRASYA METRO GRUBU J/V (2008) - *Kadikoy-Kartal Subway – Supplementary Construction and Supply, Assembly and Commissioning of Electro Mechanical Systems.* Working documentation.

BARLA G., BARLA M., PERINO A., PRINIRPITO M. (2008) - *Soluzioni analitiche e numeriche nella progettazione sismica delle opere in sotterraneo*. Proceedings of the XII MIR, pp 335-357, Torino.

BERESNEV I. and ATKINSONS G. (1997) - *Modeling Finite Fault Radiation from the ωn Spectrum.* Bulletin of the Seismological Society of America, vol. LXXXVII, pp. 67-84.

Bieniawski Z.T. (1973) “Engineering classification of jointed rock masses”, Trans S. Afr. Inst. Civ. Engrs 15, 335-344.

BILOTTA E., LANZANO G., RUSSO G., SANTUCCI DE MAGISTRIS F., AIELLO V., CONTE E., SILVESTRI F., VALENTINO M.. (2007) - *Pseudostatic and dynamic analyses of tunnels in transversal and longitudinal directions*, 4th International Conference on Earthquake Geotechnical Engineering, 4ICEGE, 25-28 June, Thessaloniki, Greece.

BOORE D. M. (1983) - *Stochastic Simulation of High-Frequency Ground Motions Based on Seismological Models of the Radiated SpectrA.* Bulletin of the Seismological Society of America, vol.LXXIII, pp.1865-1894.

BOUCHON M. (1979) - *Discrete Wave Number Representation of Elastic Wave Fields in Three-Dimensional Space*. Journal of Geophysical Research, vol. LXXXIV, no. B7, pp. 3609-3614.

BUCKLE I. A. (1996) - *Overview of Seismic Design Methods for Bridges in Different Countries and Future Directions*. Paper No. 2113, 11 WCEE, Acapulco, Mexico.

CALTRANS (1999) - *Bridge design specificationS.* California Department of Transportation.

CARRANZA-TORRES C. AND FAIRHURST C. (2000) “Application of convergence-confinement method of tunnel design to rock masses that satisfy the Hoek-Brown failure criterion”, Tunnelling and Underground Space Technology; 15: 187-213.

CARRANZA-TORRES C. (2004) “Elasto-plastic solution of tunnel problems using the generalized form of the Hoek-Brown failure criterion”, Int J Rock Mech Min Sci. 4: supplement 1, 629-639.

ERDIK M., DURUKAL E., SIYAHI B., ŞESETYAN. K. P. (2008) - *Preliminary determination of the design basis ground motions for the Istanbul Kadikoy-Kartal railed mass transport system*. Boğaziçi University. Kandilli Observatory and Earthquake Engineering, Report for the Avrasya Metro Grubu J/V.

EUROCODE 8 (2003) - *Design of Structures for Earthquake Resistance*, Draft No. VI, European Committee for Standardization, Brussels.

GEODATA SpA, (2009) - *Kadikoy – Kartal Subway, Conventional Tunneling Engineering and Design Services*, Preliminary and Final Design documentations.

GUGLIELMETTI V., GRASSO P.G., XU S. (2007) - *Mechanized Tunnelling in Urban Areas*. Taylor & Francis.

HASHAHSH Y.M.A., HOOK J.J., SCHMIDT B., YAO J.I.C., (2001) - *Seismic design and Analysis of underground structure*. Tunnelling and Underground space Technology, Vol. XVI, No.4, pp147-293, San Francisco, CA, USA.

HOEK E., KAISER P.K. AND BAWDEN W.F. (1995) “Support of Underground Excavations in Hard Rock”. Balkema, Rotterdam, 215 pp.

HOEK E. AND E. T. BROWN (1997) “Practical estimates of rock mass strength”, International Journal of Rock Mechanics and Mining Sciences. 34(8), 1165-1186.

HOEK E. AND MARINOS P (2000) “Predicting tunnel squeezing problems in weak heterogeneous rock masses”, Tunnels and Tunneling International, November, pp.45-51

IBC (2003) - *International Building Code*, International Code Council, USA.

JRA (1996) - *Japan Road Association*, Part V Seismic Design, Design Specifications of Highway Bridges. Tokyo:Maruzen, 1996

KAWASHIMA K., (2000) - *Seısmıc Desıgn of Underground Structures in Soft Ground*. Geotechnical Aspects of Underground Constructıon in Soft Ground: Proceedings of International Symposium on Geotechnical Aspects of Underground Construction in Soft Ground, IS-Tokyo’99, Japan , 19-21 July 1996, Balkema, Netherlands.

KONTOE, ZDRAVKOVIC, POTTS, MENKITI (2008) - *Case stuffy on seismic tunnel response.* Canadian Geotechinical Journal 45:1743-1764.

ISTANBUL METROPOLITAN MUNICIPALITY (2008) - *Kadikoy-Kartal Subway – Supplementary Construction and Supply, Assembly and Commissioning of Electro Mechanical Systems.* Tender documents.

MINDEVALLI O, B. MITCHELL (1989) - *Crustal structure and possible anisotropy in Turkey from seismic surface wave dispersion*, Geophys. J Int., 98, 93-106.

National Project for Design, Tendering and Construction Standards in Underground Works promoted by AGI, GEAM, IAEG, ITCOLD, SIG, SIGI (1997): "Guidelines for Design, Tendering and Construction of Underground Works" - Attachment of "Gallerie e Grandi Opere Sotterranee", No.51.

NEHRP (1997) - *Recommended Provisions For Seismic Regulations For New Buildings and Other Structures.* FEMA-303, Prepared by the Building Seismic Safety Council for the Federal Emergency Management Agency, Washington, DC.

NEHRP (2003) - *Recommended Provisions For New Buildings And Other Structures*. FEMA-450, prepared by the Building Seismic Safety Council for the Federal Emergency Management Agency, Washington, DC.

O'ROURKE M.J. & LIU X., (1999) - *Response of buried pipelines subject to Earthquake effects.* Monograph No.III, MCEER (Multidisciplinary Center for Earthquake Engineering Research) Publications, University at Buffalo, Red Jacket Quadrangle, Buffalo, NY 14261..

PALMSTROM A. (1996) "Characterizing rock masses by the RMi for use in practical rock engineering", Tunn. and Und, Space Tech. vol.11.

PAOLUCCI R., PITIKALIS K., (2007) - *Seismic risk assessment of underground structures under transient ground deformation*. In Pitikalis, K. (editor). Earthquake Geotechnical Engineering. Chapter 18, pp 433-459. Springer-Vienna.

PECK R.B. (1969) - *Deep Excavation and Tunneling in Soft Ground*. Proceedings of the VII International Conference Soil Mechanics and Foundation Engineering, Mexico, State of the art volume, State of the art Report, pp. 225-290.

POWER M.S., ROSIDI D., KANESHIRO J., (1996) - *Strawman: screening, evaluation, and retrofit design of tunnels. Report Draft.* Vol. III, National Center for Earthquake Engineering Research, Buffalo, New York.

RUSSO G, KALAMARAS G.S. AND GRASSO P. (1998) "A discussion on the concepts of geomechanical classes, behavior categories and technical classes for an underground project", Gallerie e grandi opere sotterranee, N.54, pp.40-51.

RUSSO G. AND GRASSO P. (2006) "Un aggiornamento sul tema della classificazione geomeccanica e della previsione del comportamento allo scavo", Gallerie e grandi opere sotterranee, N.80, pp.56-65.

RUSSO G. (2007) "Improving the reliability of GSI estimation: the integrated GSI-RMi system", ISRM Workshop, Underground Works under Special Conditions, Madrid, 6 July.

RUSSO G. AND GRASSO P. (2007) "On the classification of rock mass excavation behaviour in tunnelling", 11th Congress of International Society of Rock Mechanics ISRM, Lisbon.

ST. JOHN C.M. & ZAHARAH T.F., (1987) - *A seismic Design of Underground Structures*. Tunneling and Underground Space Technology, Vol.II, Issue 2, pp.165-197, Pergamon, U.K.

TZAMOS S. AND SOFIANOS A. (2007) "A correlation of four rock mass classification systems through their fabric indices", International Journal of Rock Mechanics and Mining Sciences .

UNION INTERNATIONALE DES CHEMINS DE FER (2002) "UIC-Codex 779-9R - Safety in Railway Tunnels", 24 September 2002.

WANG J.N., (1993) - *Seismic design of tunnel – A simple state of the art design approach*. Parson Brinckerhoff Quade & Douglas, Inc., New York, Monograph 7.